NTNU
Kunnskap for en bedre verden

Department of Engineering Cybernetics

TTK4900 - Master project

Retrofitting a legacy robotic arm using open-source solutions

Author:
Kristian Blom

07.06.24

Table of Contents

List of Figures

List of Tables

1 Preface

2 Introduction

2.1 Purpose

This report describes the master thesis project conducted by Kristian Blom during the spring semester of 2024. The project builds directly on the specialisation project concluded the previous semester of autumn 2023. This report contains relevant excerpts from the specialisation project report.

2.2 Background and motivation

From the initial project description: *This project is defined and commissioned by a student in co-operation with Omega Verksted (OV). It builds on the specialisation project named "From hardware to control algorithms: Retrofitting a legacy robot using open source solutions", in which new control hardware was developed for an old robotic arm. The arm is a 6DOF industrial arm originally developed for chemical analysis and consists of a 5DOF arm with a pincer/manipulator installed on a rail. The developed hardware controls 6 brushed DC motors and processes information from 6 incremental encoders, 6 current sensors, 3 accelerometer/gyroscope units, 2 optocouplers and 1 mechanical switch.*

This document is not just a thesis, but also intended for people with less experience, and the language generally tries to reflect that

2.3 Project scope

The primary goal of this project has been to develop a robotic software system compatible with hardware developed during the specialisation project, such that the robotic arm may be operated by a non-expert third party. The primary use case is the mixing of beverages during informal meetings at Omega Verksted. The secondary goal of the project is that the software system should be readily expandable to support more sophisticated use cases and sensors, such as 3D printing and robotic vision, by an expert third party.

Project scope as itemised list:

1. Implement and verify required hardware improvements from the specialisation project.
2. Write hardware drivers for the relevant microcontroller peripherals.
3. Develop and implement a software architecture around the primary and secondary goals of the project.
4. Develop and implement tests to evaluate the system's performance.

3 Abbreviations and glossary

4 System specification

This section provides a high level description of the robotic system(4.1), a description of the hardware developed during the specialisation project(4.2), and a requirement specification for the software developed in this master project(4.3). The latter elaborates on scope items 2 and 3 from section 2.3.

4.1 Overview

The system consists of a robotic arm known from the original manufacturer, Beckman Coulter, as Optimized Robot for Chemical Analysis (ORCA); hardware developed as part of the specialisation project; and a general purpose desktop computer running the Linux/Ubuntu operating system. The arm is actuated by 6 DC motors, each connected to one joint via belts and gears within the arm. The arm is illustrated in figure 1, annotations marking each joint's positive direction. The gripper is mounted on a linear actuator, and is designed to bend around an object placed near the middle. It is capable of lifting and manipulating objects of approximately one kilogram.

The arm has several "hardpoints" on which PCBs or other equipment may be mounted, named after their physical location on the arm. The three control units developed in the specialisation project are mounted on the torso, shoulder and hand hardpoints, respectively. They are each responsible for the control of two joints, named after their function and/or physical location. For instance, the shoulder control unit is mounted on the shoulder hardpoint, and is responsible for controlling the elbow and wrist joints. A high level overview of the robotic system is presented in figure 2.

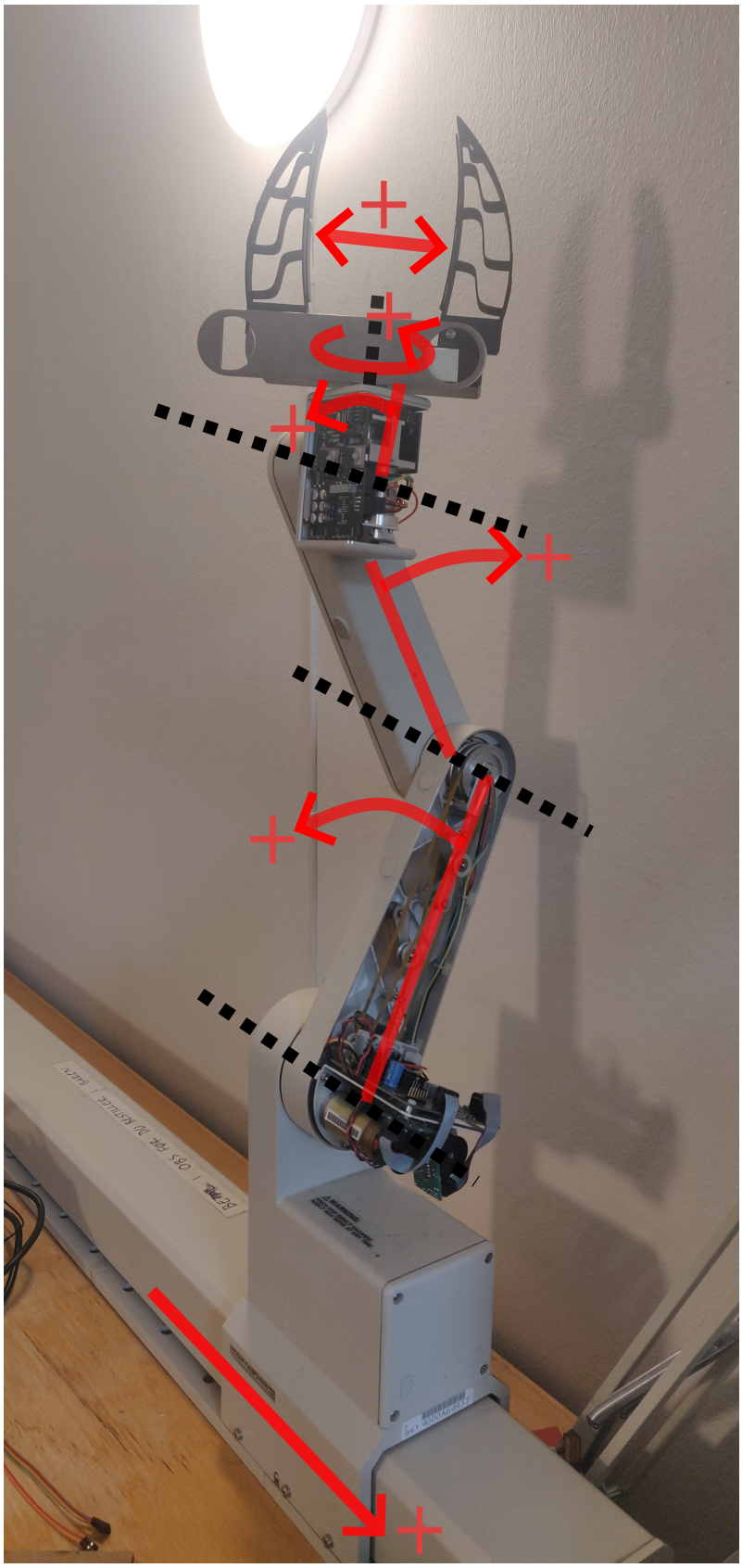

Figure 1: The ORCA arm, illustrated with joints and their directions. From the bottom up, joints are named rail, shuolder, elbow, wrist, twist and pinch.

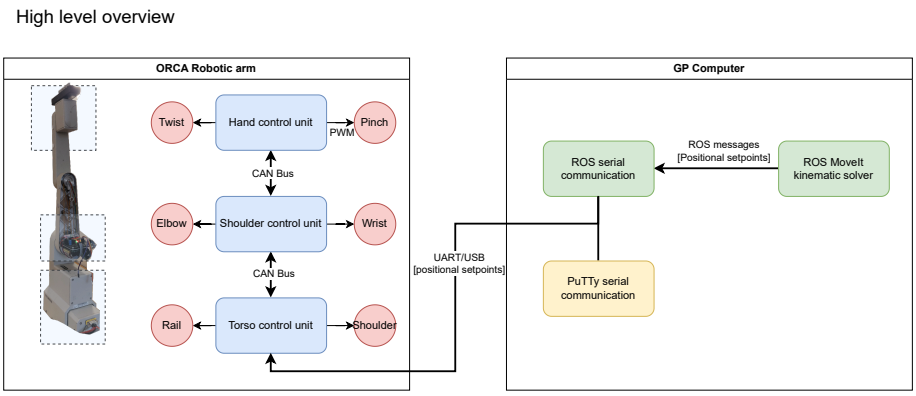

Figure 2: An overview of the robotic system

4.2 Hardware

As mentioned in section 2.2, all mechanical and some electromechanical parts were kept during the specialisation project in order to limit its scope. The parts are presented in table 1, originally presented in the specialisation project report. These parts were all found to be in working order, and replacing them would have required modification of the arm chassis.

For an in-depth discussion and presentation of the hardware, see sections 6 and 7 of the specialisation report. A key point from those sections is that there are space limitations in the arm preventing IMUs from being placed such that they may interface with their respective joint controllers directly. As a consequence, a critical function of the CAN bus is to enable transmission of IMU data between control units.

The following subsections explain each PCB developed in the specialisation project, and are summarised in figure 3. Figure 4 provides a detailed description of the arm, and was originally presented in the specialisation project report[2].

Table 1: Original parts kept in the project

Part name	**Description**	**Part no.**
Rail motor	Pittman 40mm 30.3V BDC motor	9233C59-R1[9]
Shoulder motor	Pittman 54mm 30.3VDC BDC motor	14205C389-R1[10]
Elbow motor	Pittman 40mm 24V BDC motor	9234C59-R1[9]
Wrist motor	Pittman 30mm 30.3V BDC motor	8224C143-R2[8]
Twist motor	Escap 23mm 23LT2R, 12V BDC motor	23LT2R[5]
Pinch motor	Escap 23mm 23LT2R, 12V BDC motor	23LT2R[5]
Wrist rotational sensor	TT Electronics Photologic Slotted Optical Switch	OPB971N51[4]
End switch	TT Electronics Photologic Slotted Optical Switch	OPB971N51
Motor encoder	Optical quadrature encoder 500CPR	HEDS-9100[17]

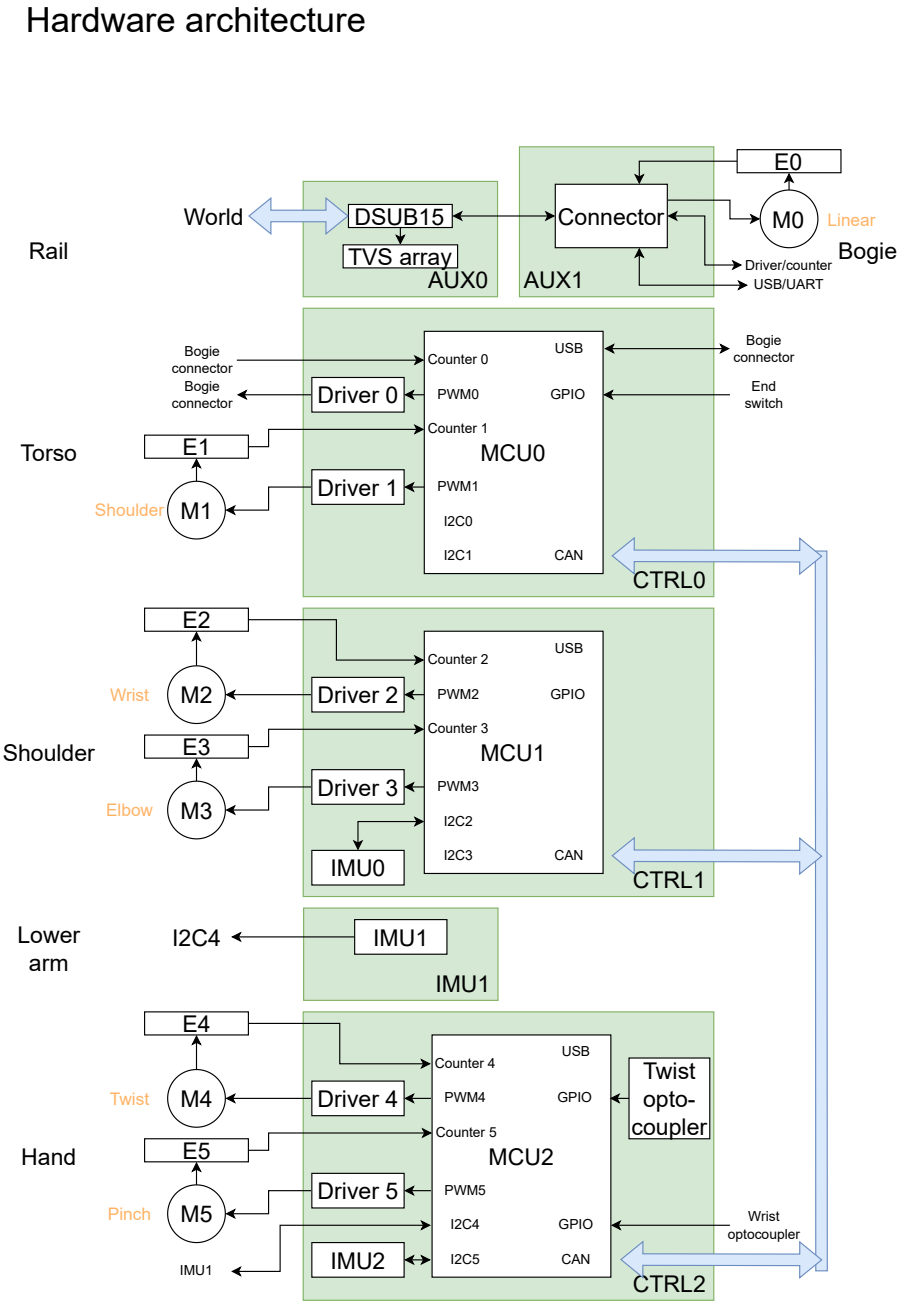

Figure 3: Hardware architecture. Green squares represent a PCB designed in the specialisation project, with key components as white squares. Left hand keywords indicate PCB mount location inside the arm. Originally presented in the specialisation report.

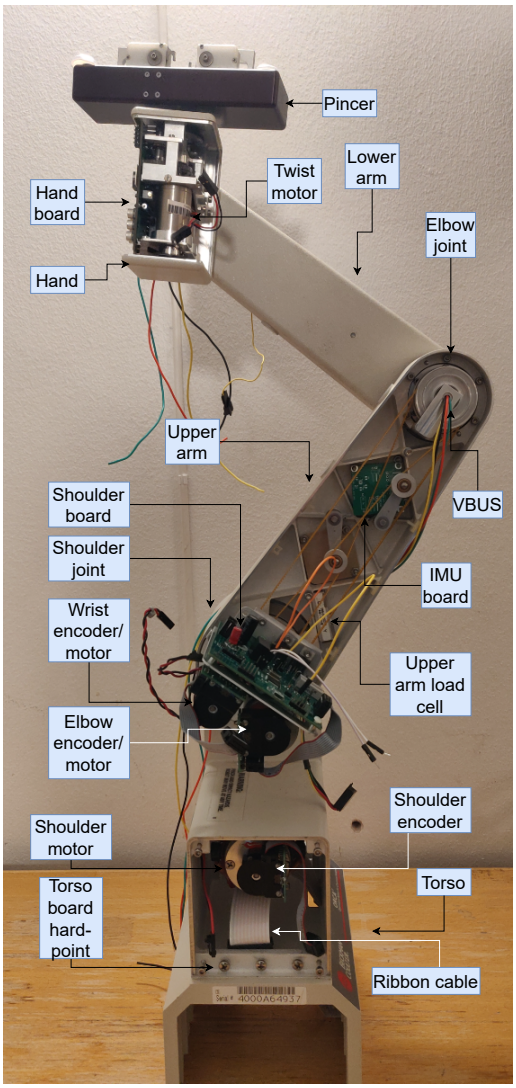

Arm viewed from the front.

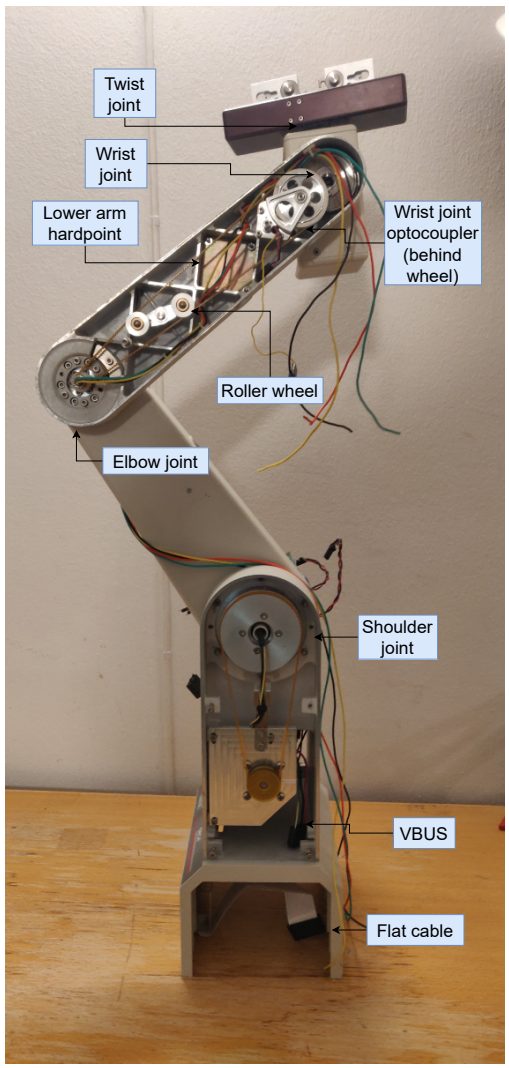

Arm from the back.

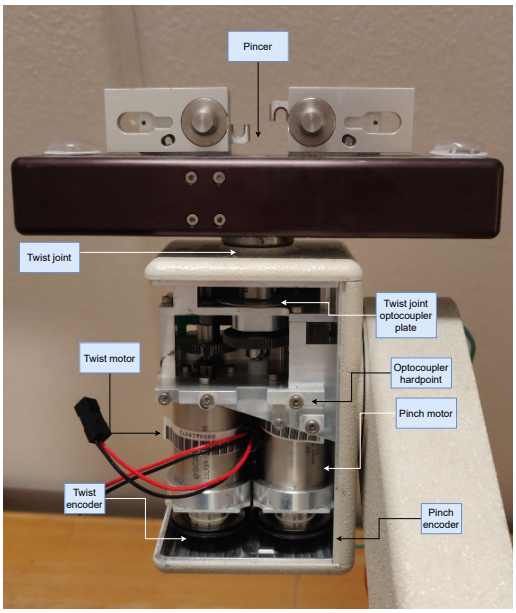

A more detailed image of the hand and pincer.

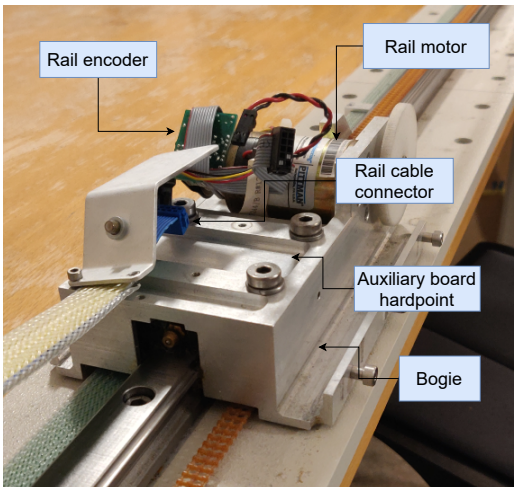

The bogie on which the torso is mounted.

Figure 4: The arm with annotations. Orginally presented in the specialisation report

4.2.1 Auxiliary 0: Rail

The rail PCB is responsible for the arm's interface, a DSUB15 connector with signals for USB, UART and power. It is mounted on the rail hardpoint, and provides a socket for the 16 wire ribbon cable through which it interfaces with the bogie PCB(4.2.2). Additionally, it protects the USB and UART data lines from voltage spikes via its TVS array CDSC706[3]. The TVS array is clamped at 5V sourced from the torso control unit(4.2.3).

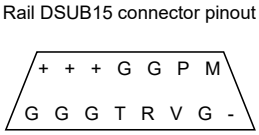

Figure 5: DSUB15 pinout

Table 2: Legend for figure 5, DSUB15 connector

Legend	**Meaning**
+	Input voltage
G	Ground
P	USB_DP
M	USB_DM
T	UART Tx
R	UART Rx
V	USB_VBUS
-	Not connected

4.2.2 Auxiliary 1: Bogie

The bogie PCB provides sockets for the 16 and 20 wire ribbon cables, as well as the rail motor and encoder connectors. Its purpose is to bundle the 16 wire ribbon cable with the rail motor and encoder wires into the 20 wire ribbon cable, through which it interfaces with the torso control unit(4.2.3).

4.2.3 Control unit 0: Torso

The torso control unit is responsible for the control of the rail and shoulder joints via motor 0 and motor 1 respectively, as well as external communication via the USB/UART lines. It interfaces with the upper arm IMU, IMU0 (4.2.4), via the shoulder control unit and the CAN bus. IMU0 is used in conjunction with E1 for the estimation of shoulder joint position. See table 3 for a presentation of the symbols in figure 3.

4.2.4 Control unit 1: Shoulder

The shoulder control unit is responsible for the control of the elbow and wrist joints via motors 2 and 3 respectively. It interfaces with the lower arm and hand IMUs, IMU1 and IMU2, via the hand control unit (4.2.6) and the CAN bus, for control of the elbow and wrist joints in conjunction with encoders 2 and 3, respectively. Additionally, it is responsible for direct communication with IMU0 via I2C. For remaining items, see table 3.

Table 3: Control unit 0

Symbol	Description	Unit name
Encoder 0 (E0)	Registers movement in the rail motor, used in estimation of the rail joint position. Relative, quadrature	HEDS-9100
Encoder 1 (E1)	Shoulder motor, see E0	HEDS-9100
End switch	Optical sensor, detects linear rail end position	See table 1
Driver 0	Motor driver, supplies power to the rail motor and provides current draw output. PWM control, analog current mirror	DRV8251A
Driver 1	Shoulder motor, see driver 0	DRV8251A
IMU0	Upper arm IMU	LSM6DSM
Microcontroller 0 (MCU 0)	Processing unit for control unit 0	STM32F303
Motor 0 (M0)	Linear rail motor, brushed DC	See table 1
Motor 1 (M1)	Shoulder joint motor	See table 1

4.2.5 IMU board 1: Lower arm

The IMU board serves as a mount point for the lower arm IMU, IMU1, which is used in the estimation of elbow joint position, and interfaces with the hand control unit via I2C. The IMU board also interfaces with the wrist optical sensor, relaying 5V from the hand control unit and sensor output to the hand control unit. IMU board 1 is mounted on the lower arm hardpoint.

4.2.6 Control unit 2: Hand

The hand control unit is responsible for the control of the twist and pinch joints via motors 4 and 5 respectively. It interfaces with the twist optical sensor and the wrist optical sensor via GPIO interrupts, and the CAN bus. Additionally, it is responsible for direct communication with IMUs 1 and 2 via I2C.

The twist optical sensor activates when the twist joint is in one specific position. As the twist joint has no hardpoints on which an IMU may be mounted, this sensor is essential to the estimation of twist joint position.

The wrist optical sensor activates for a set of joint positions, and may be used in the estimation of wrist joint position.

For remaining items, see table 3.

4.3 Software

The hardware presented in section 4.2 provides constraints for the software architecture. As mentioned, the software covers scope points 2 and 3 from section 2.3. This section elaborates on the functional requirements of the system, and presents a requirement specification which the finished software should fulfill.

Some keywords must be defined in the context of the requirement specification:

Must, shall: Denote a requirement which the failure to heed would significantly compromise the system's ability to achieve the project's two goals.

Should: Denotes a requirement which the failure to heed would only reduce the system's ability to achieve the project's two goals

4.3.1 Functional analysis

The primary goal for the system is to be able to "mix beverages" in informal settings, and be useable by non-expert personnel. This involves manipulating glasses, bottles and other objects that would typically fit in a human hand[1]. In order to achieve this, the system must implement the following functions:

- F1: Control the position and orientation of the pincer with an accuracy such that it may manipulate objects commonly involved with the mixing of beverages
- F1.1: Control the position of 6 joints concurrently
- F1.2: Take positional setpoints from a source external to the arm

"Informal settings" imply the presence of personnel and equipment which may not be accustomed to or intended for working with a robotic system during operation. Non-expert personnel refers to persons who may be familiar with robotic or autonomous systems in general, but do not have intimate knowledge of this system. In order to ensure safe operations in such a setting, the system should implement the following functions:

- F2: Operate in a predictable manner
- F2.1: Avoid fast or jerking motions
- F2.2: Follow predictable and/or intuitive movement patterns
- F3: Detect and respond when safe operational parameters are exceeded
- F4: Provide a user interface which requires limited preparation and/or education to make use of.

4.3.2 Architectural requirements

The secondary goal for the system is that it should be readily expandable to support use cases requiring a higher degree of movement accuracy, and/or more advanced sensors than currently exist within the hardware, by expert personnel. Expert pesonnel refers to persons who are experienced with robotic systems and embedded programming. This puts constraints on the development of the system's architecture:

- AR1: The system should consist of clearly defined modules
- AR1.1: A module's interface should be clearly defined
- AR1.2: A module should be limited in scope and purpose
- AR1.3: It should not be possible to pass information to a module outside of its interface.
- AR1.4: Naming conventions should apply across modules
- AR2: The system should adhere to common standards and best practices for embedded programming
- AR2.1: SOLID principles should be adhered to, to the extent that they apply
- AR2.2: Modules should aim for low coupling and high cohesion
- AR3: Design patterns should apply across modules

[1] This is a postulate

4.3.3 Documentation requirements

The secondary goal, as well as this being a master thesis project, sets expectations for code documentation:

- DR1: All modules should be documented
- DR1.1: All functions, classes, structs et cetera should have unique documentation
- DR2: Documentation should be readily available
- DR3: Documentation conventions should apply across modules
- DR3.1: Language should be similar across modules

5 Theory

SOLID Coupling and cohesion, other relevant concepts CAN UART TVS arrays, voltage clamping Switching vs linear voltage regs Interrupts

5.1 Inter-integrated circuits (I2C)

5.2 Software development

5.3 Communication protocols

Message round trips vs bitrates

5.4 Circuit design

6 Tools and workflow

This section describes the tools used in the project, for the purpose of reproduction and/or future development.

6.1 Software

6.1.1 Tools

KiCad 7, CERN distro[SOURCE] was used in the development of PCBs in the project's initial phase, without non-standard plugins. KiCad is an open source, freely available CAD software for the design of PCBs. When necessary, component footprints were downloaded from the UltraLibrarian[SOURCE] website when available, or otherwise drawn in KiCad based on component datasheets. These footprints may be found in FOLDER.

Git was used during all phases of the project, and the project's repository may be found at Github[SOURCE].

STMCubeMX[SOURCE] was used for the initialisation of microprocessor peripherals, i.e. the generation of peripheral drivers, and the generation of the project's Makefile. STMCubeMX is a configuration tool published and maintained by ST, the manufacturer of the STM microprocessor family, providing a GUI through which the user may create a pinout, enable interrupts et cetera for their microprocessor. It is freely available, but requires the registration of a user account with ST[SOURCE]. The tool generates .h and .c files for the relevant peripherals based on choices made in the GUI, as well as either a Makefile for use with development tools outside the ST software ecosystem, or the equivalent for use with ST's own STMCubeIDE IDE. This project utilised the Makefile option as it seeks to minimise the use of non-open-source solutions.

VSCode[SOURCE] with ST extension[SOURCE] was the primary IDE for this project. The extension *stm32-for-vscode* was used to build and flash binaries for the MCUs.

PuTTy was used for serial communication with and debugging of the MCUs.

ROS2 Iron

MoveIt

6.1.2 Workflow

MCU binaries:

- Set peripheral configuration parameters in STMCubeMX
- Ensuring that the "overwrite user code" option is unchecked, generate code.
- Edit generated files as necessary, ensuring code is added between USER CODE labels to avoid being overwritten the next time STMCubeMX is used to generate/update peripheral settings.
- Add and edit source files in the TTK4900_drivers folder under the root folder created by STMCubeMX.
- Ensure source files are registered in the Makefile generated by STMCubeMX.
- Build binary file using the ST extension in VSCode.
- Flash binary to MCU using the ST extension and ST-LINK unit embedded in the development kit6.2.

ROS nodes

- Do stuff

6.2 Electronic/Hardware

6.3 Mechanical

- KiCad
- Git
- ST CubeMX
- VSCode (extensions: ST, C/C++)
- Development kit
- Angular measurement tool
- Power source
- Oscilloscope
- MoveIt
- Putty
- Categories: Electr(on)ic, Software, Mechanical
- Fusion 360
- Prusa Slicer

7 Hardware improvements

This section summarises key points from the implementation of the hardware improvements mentioned in the Further work chaper of the specialisation report, dubbed Mk1.1. PCBs produced for the specialisation project are dubbed Mk1. For a detailed presentation of the hardware and its functions, see chapters 6 and 7 of the specialisation report in APPENDIX. The relevant copper layers are presented in each subsection as a visual reference for pin headers/connectors, while all circuit schematics are collected at the end of the section.

Additionally, this section discusses results from the verification of Mk1.1 hardware. As they lay the foundation for the master project they are not considered "results" of the master thesis as such, and will only be adressed to the extent to which they affected the project's software implementation in section 15.

7.1 Improvement matrix

Table 4 summarises the "Further work" section of the specialisation report[2] and was originally presented there. Each entry in the left column represents a point of improvement, and a cross in a subsequent column indicates that the issue affects the hardware unit in the top row of that column.

Table 4: A summary of further work

Item/affects unit	**Hand**	**Shoulder**	**Torso**	**Bogie**	**Rail**	**IMU (board)**	**MCU**
USB VBUS voltage divider		X	X				
USB VBUS pin		X	X				X
USB pullup on DM		X	X				
USB pullup transistor		X	X				
IMU 5V and 3.3V lines	X	X				X	
IMU/OPT header design	X	X				X	X
IMU header placement		X					
CAN verification	X	X	X				
CAN/48V connector placement			X				
CAN transciever placement	X						
Nylon bolts	X						
Mount point placement		X	X		X		
Mount point size		X	X				
20 pin connector			X	X			
Motor driver to PWM output	X	X	X				X
Motor driver ADC/PWM							X
Motor driver header silk	X						
Optocoupler 5V	X					X	X
Wrist optocoupler function	X					X	X
Bulk cap/pin header swap	X						
1.27mm jumpers	X						
Switching regulators	X	X	X				
Horisontal voltage regulators			X				
Voltage regulator LED resistor	X	X	X				
Encoder circuits							
Encoder header rotation				X			
TVS array					X		
Motor driver relay control		X	X				
Motor characterisation							
PCB production	X			X	X		

7.2 MCU pinout

The MCU pinout lays the foundation for layout of the PCBs, and was therefore changed first. The pinout is presented in figure 6.

- USB VBUS detection was set to pin PA9 in accordance with AN4879 chapter 2.6[12].
- PA10 was set to output as USB DP driver in accordance with AN4879 figure 5.
- PB12, PB13, PC10 and PC11 were opened as interrupt inputs to accommodate optical switches and IMU programmable interrupts, as well as ensuring optical sensor inputs are placed on 5V tolerant pins according to table 13 ofthe MCU datasheet[15].
- PWM output for motor driver 2 was moved to PC1 and PC2 from PC6 and PC7 in order to simplify PCB layout by gathering all motor driver outputs along one edge of the MCU.
- Current sense ADC input for motor driver 2 was moved from PA0 to PC3 in order to avoid an interference mode between peripherals, see elaboration below.

A key finding from the specialisation project was the discovery of an interference mode between the TIM2 (timer 2) and ADC1 peripherals[2], see chapter 13.3[2]. When TIM2 was configured for PWM generation, and ADC1 was activated on pin PA0, PA0 acted as an output pin with an analog voltage output proportional to the PWM duty cycle on TIM2. The cause of the interference mode could not be established beyond the fact that PA0 may also be configured for output from TIM2. As a workaround, ADC1 was moved to pin PC3, which is not compatible with TIM2. Additionally, TIM2 was not used for PWM generation. For more information about timer configuration, see section 8.8.

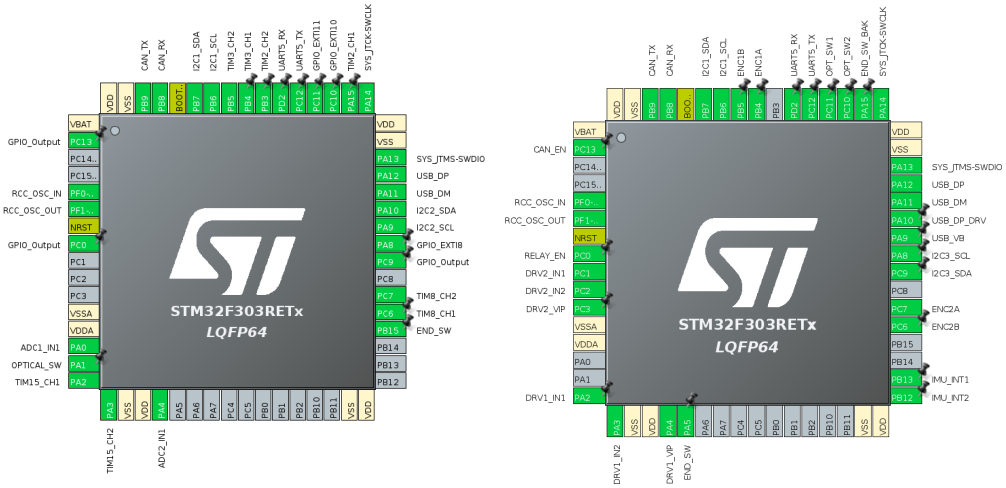

MCU pinout configuration prior to hardware improvements

MCU pinout configuration after hardware improvements

Figure 6: Comparison of the old and new MCU pinout configuration

7.3 IMU board

As mentioned in section 4.2, the IMU boards act primarily as mounting points for the IMUs, and were to be mounted on hardpoints in the upper and lower arm sections, see figure 4. Secondarily, the lower arm IMU board would act as an interface with the wrist optical sensor. The LSM6DSM IMU has two configurable interrupt output pins[13] in addition to its I2C interface, and it was decided that at least one of these should be available for use in the system.

[2]The report mentions pin PA4. This is erroneous; the interference was present on pin PA0

The OPB971 optical sensor requires an input voltage of minimum 4.5V[4], while the LSM6DSM IMU has a maximum input voltage of 3.6V[13]. In order to save space in the wrist joint hole, it was decided that only the 5V line should be pulled from the hand control unit rather than both 3.3V and 5V lines. This necessitates a conversion from 5V to 3.3V in order to safely power the IMU. A key failure of the specialisation project IMU board design was the use of a voltage divider for stepping down the voltage, and a dedicated 3.3V step-down converter was introduced to amend this: the ZMR330, which outputs 3.3V for an input voltage between 4.8V and 24V[7].

Figure 7 shows the improved IMU layout. Several headers/jumpers have been introduced to accommodate the various signal output options, and the PCB's interface header **I2C_PWR1** has been reduced from 8 to 6 pins compared to the specialisation project design (see chapter 9.8 of the report[2]). Jumper **INT_SEL1** lets the user select IMU interrupt 1 or 2 for output to the hand control unit. Jumper **INT_EN1** lets the user select whether or not to send the selected interrupt to output. The two jumpers implement the following boolean function:

$$I_{I2C\_PWR1} = (1_{INT\_SEL1} \oplus 2_{INT\_SEL1}) \cdot (I_{INT\_EN1} \oplus O_{INT\_EN1}) \tag{1}$$

If **INT_EN1** is set to O, the interrupt selected by **INT_SEL1** will be grounded. The other interrupt will be left floating.

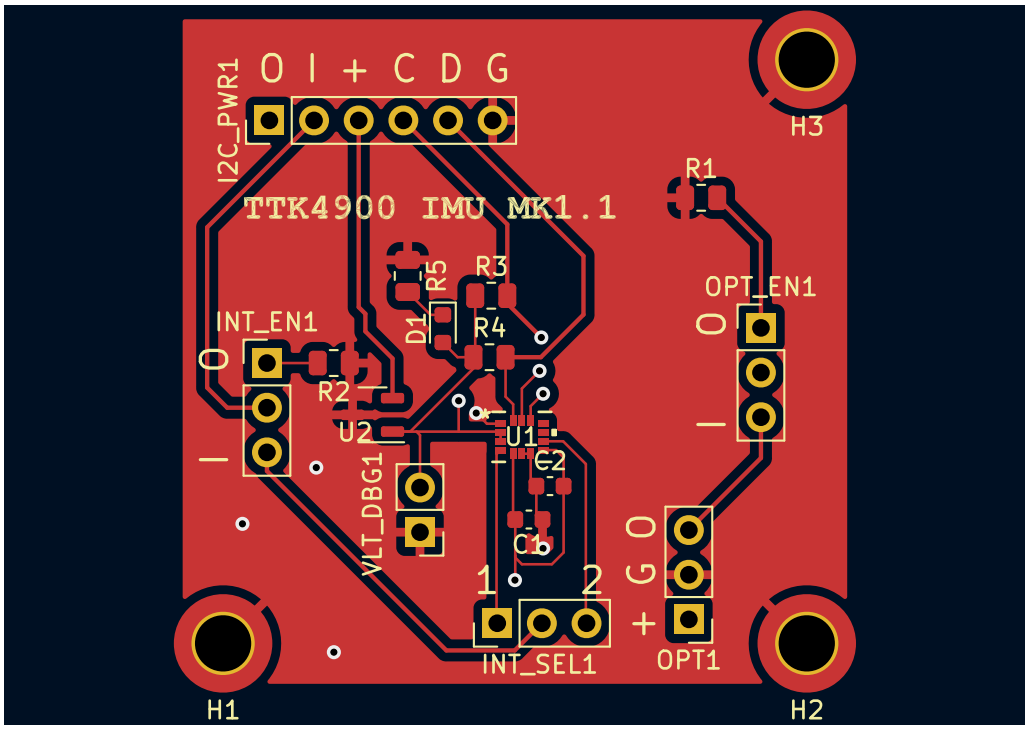

Figure 7: Front copper and silk layers of the improved IMU board

7.4 Rail

New measurements for all mount holes were taken by laying the original rail board on millimeter paper and drawing the outline of the board and inline of the mount points using a 0.5mm graphite pencil. This provided a higher accuracy with respect to finding the mount point centra relative to the board outline than using a caliper, which was the tool used in the specialisation project.

The specialisation report suggests replacing the CDSC706 TVS array with one capable of protecting all 14 lines entering the arm. This was elected against due to uncerainty regarding correct clamping

Table 5: IMU board header pin legend

I2C_PWR1	**Meaning**	**OPT_EN1**	**Meaning**
O	Optical output	I	Optical sensor output enable
I	IMU interrupt output	O	Optical sensor output disable
+	5V in	**OPT1**	**Meaning**
C	I2C Clock	+	Optical sensor 5V input
D	I2C Data	G	Optical sensor ground
G	Ground	O	Optical sensor output
INT_EN1	**Meaning**	**INT_SEL1**	**Meaning**
O	Disable IMU interrupt output	1	IMU interrupt 1 select
I	Enable IMU interrupt output	2	IMU interrupt 2 select
VLT_DBG1	**Meaning**	-	-
3.3V	output debug	-	-

and the unprotected lines to some extent being protected by diodes on the control boards (see section 8.2.1 of the specialisation report).

Table 6 explains the silk symbols on the 16 pin connector socket of the rail board as seen in figure 8, which shows the back copper and silk of the rail board. The silk should be interpreted as an overlay of the pins, such that the label "5" corresponds with connector pin 8. The 14 pin header on the upper right of figure 8 is connected to the DSUB15 connector presented in section 4.2, silk symbols explained in table 2.

Note: The input voltage pins were initially left partially unconnected due to a design error. This was corrected, and the rail version number was elevated to 1.2.

Table 6: Rail board 16 pin connector

16 pin connector	**Meaning**
G	Ground
P	USB_DP
M	USB_DM
V	USB_VBUS
R	UART Rx
T	UART Tx
5	TVS 5V clamping
+	Input voltage

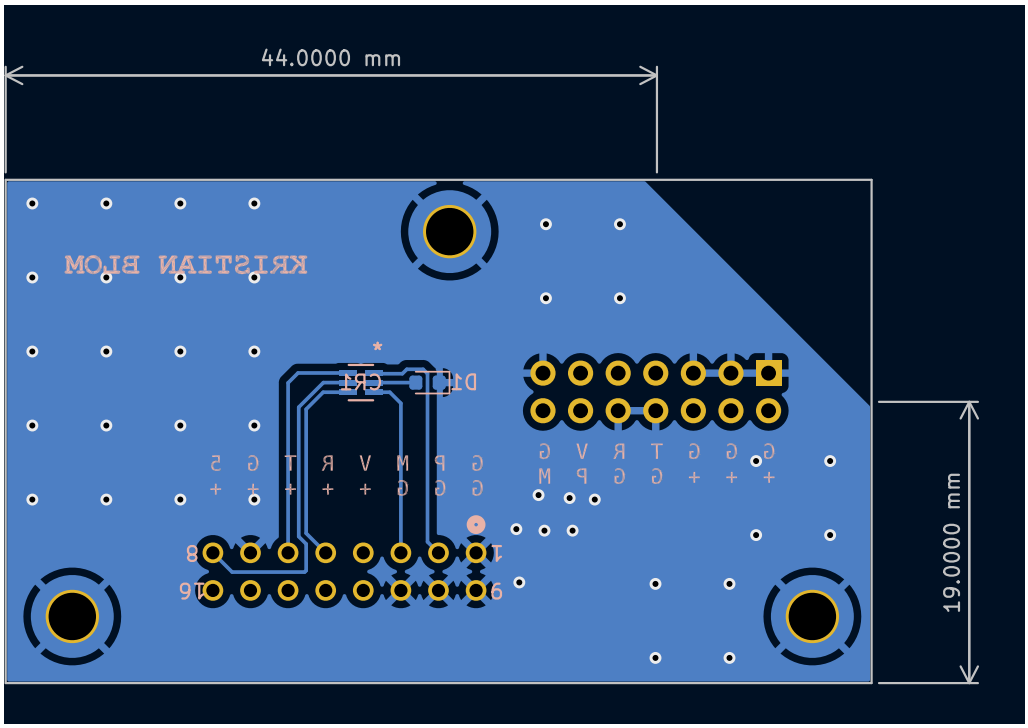

Figure 8: Back copper and silk layers of the improved rail board

7.5 Bogie

A key error in the design of the bogie board was the pin assignment of the 20 pin connector socket through which it interfaces with the torso control unit. It was discovered that one row of pins on the connector had been mirrored compared to the pin assigment on the torso board. This in turn was due to the pin numbering schemes in the schematics of the torso and bogie circuits differing: the bogie connector used the "counter clockwise" numbering scheme, while the torso connector used the "top/bottom" numbering scheme. The bogie connector was changed to "top/bottom" in order to match the torso, which corrected the issue.

Additionally, the rail motor encoder pin header was rotated 180 degrees to better accommodate the encoder ribbon cable and connector.

The improved bogie board is presented in figure 9, and the silk symbols for the 20 pin connector socket is presented in table 7. The silk symbols for the 16 pin connector socket is presented in table 6.

Note: Finding the cause of the connector issue took two attempts, and the bogie version number is therefore 1.2.

Table 7: Bogie board 20 pin connector socket, end switch connector header

MAIN1	**Meaning**	**END_SWITCH1**	**Meaning**
ES	End switch output	G	Ground
VB	USB_VBUS	E	End switch output
DM	USB_DM	+	5V input
DP	USB_DP		
5	5V output		
B	Encoder ch B		
A	Encoder ch A		
T	UART Tx		
R	UART Rx		
G	Ground		
+	Input voltage		
M1	Motor input 1		
M2	Motor input 2		

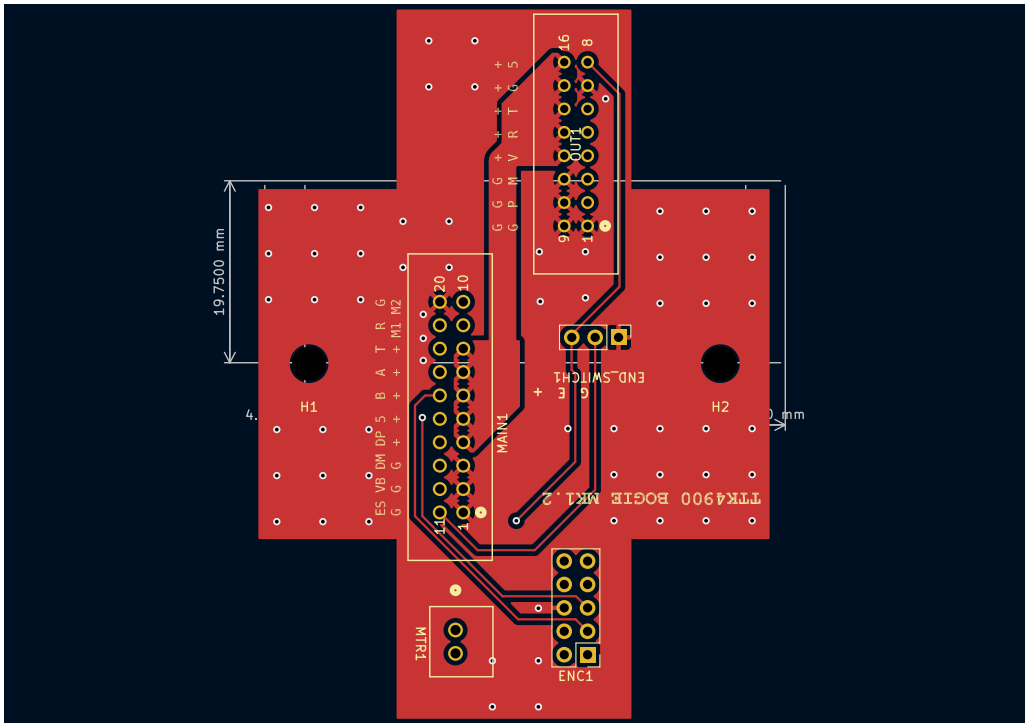

Figure 9: Front copper and silk layers of the improved bogie board

7.6 Torso

In addition to changes made uniquely to the torso, this section summarises improvements made to the various assemblies which make up the control units. Figure 11 presents the improved torso control unit. Legends for various pin headers are presented in 8.

7.6.1 USB assembly

Circuit was redesigned in accordance with chapter 2.6 and figure 5 of AN4879[12], see figure 10. R1 was set to $33k\Omega$, R2 to $82k\Omega$. The specialisation report suggests to add a transistor between PA10 (USB DP driver) and the DP line such that the MCU would not drive the line directly. However, this was deemed unnecessary on the basis that figure 5 and the following quote imply that the DP

line may be driven directly via a resistor: “A DP pull-up must be connected only when VBUS is plugged. A GPIO from the MCU is used to drive it after the VBUS detection..[...]” - Chapter 3.1.1 of AN4879.

Figure 5. **USB FS upstream port without embedded pull-up resistor in self-powered applications**

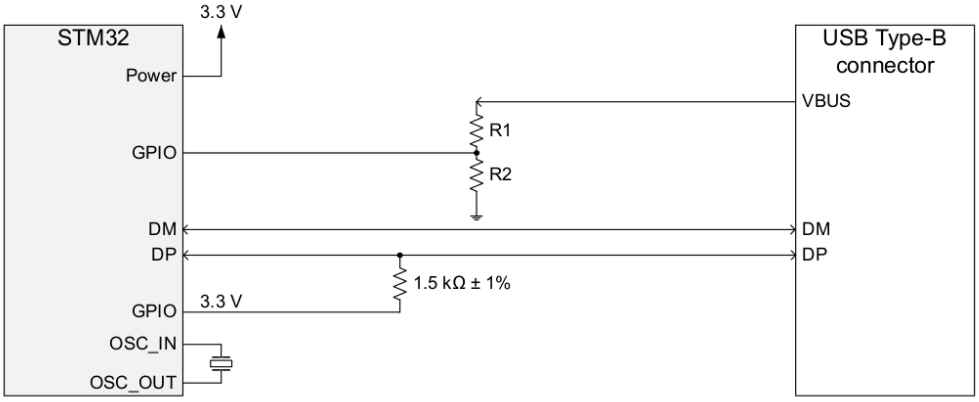

Figure 10: Figure 5 from ST AN4879, illustrating a valid USB circuit

Based on this, a $1.5k\Omega$ resistor was placed between PA10 and PA12. In order to fulfill the requirement of only connecting the DP pullup when VBUS is plugged, it was decided that an interrupt would be used to activate PA10 in software upon VBUS-detection, and that the pin would otherwise be held in its reset state.

Additionally, AN4879 chapter 2.3 recommends protecting data lines with a USBLC6 IC, which was also implemented.

7.6.2 CAN bus assembly

The CAN bus assembly/circuit was not satisfactorily verified during the specialisation project: *The CAN circuit was tested between the development kit and the MCU on the breadboard. While a correctly configured CAN message could be observed by oscilloscope on any point of the data lines, no indication was observed that the recipient MCU (breadboard) had registered the message.*(section 13.1.1)

During manufacture of the Mk1.1 units, it was discovered that the wrong CAN transciever unit had been used in the receiving unit during the specialisation project test. The intended unit was TJA1057**B**T, while TJA1057**G**T was used. The TJA1057 datasheet[11], chapter 6, specifies that pin 5 of the BT unit may be used as a voltage level adapter reference (V_{IO}) for the CAN node TXD/RXD lines such that it may utilise a voltage different from the CAN standard of 5V. This is a necessary function in this system, as the MCU voltage is 3.3V. However, pin 5 of the GT unit is not connected. BT units were salvaged from Mk1 control units and installed in Mk1.1. CAN bus was successfully tested using BT units, and the conclusion is that the GT/BT switch was the reason for the previous negative result (7.9.10)

Additionally, the CAN bus/power connector was moved towards the edge of the board in order to simplify integration with the arm.

7.6.3 Mount points

Positions and diameters of all mount points were redesigned using the same method as described in section 7.4. The diameter of holes H1 and H2 were increased 3.5mm from 2.7mm; H3, H4 and H5 were increased to 5.3mm from 2.7mm. All holes are non-plated.

7.6.4 Motor drivers

Motor driver PWM signal lines were changed in accordance with the update to MCU pinout described in section 7.2.

Additionally, a 2N551 NPN BJT transistor was chosen to actuate the JV-3S-KT relay which acts as a dead man's switch for the motor drivers. The transistor is operated from pin PC0 of the MCU, see fig 6.

7.6.5 Voltage regulators

The specialisation report suggests replacing the LM317HV[19] linear voltage regulators with an equivalent switching regulator. Two regulators on each control unit step the system input voltage down to 3.3V and 5V, respectively, in order to supply relevant ICs. The LM317HV were found to rise to a substantial temperature at an input voltage of 20V during the specialisation project, and the target input voltage for the system is 48V[3]. As switching regulators develop less heat than linear regulators, it was deemed beneficial to change from linear regulators. However, due to the limited time available for implementation of Mk1.1, this was elected against.

PCB footprints of the regulators were changed to horisontal from vertical, in part to improve heat dissipation by using the PCB itself as a heat sink, and in part to make placement of the regulators independent of the mount points available on the external heat sink.

Additionally, the output voltage indicator LED resistor was increased from 200Ω to 1.5$k\Omega$ in order to dim the LEDs and reduce eye strain when working with the control units.

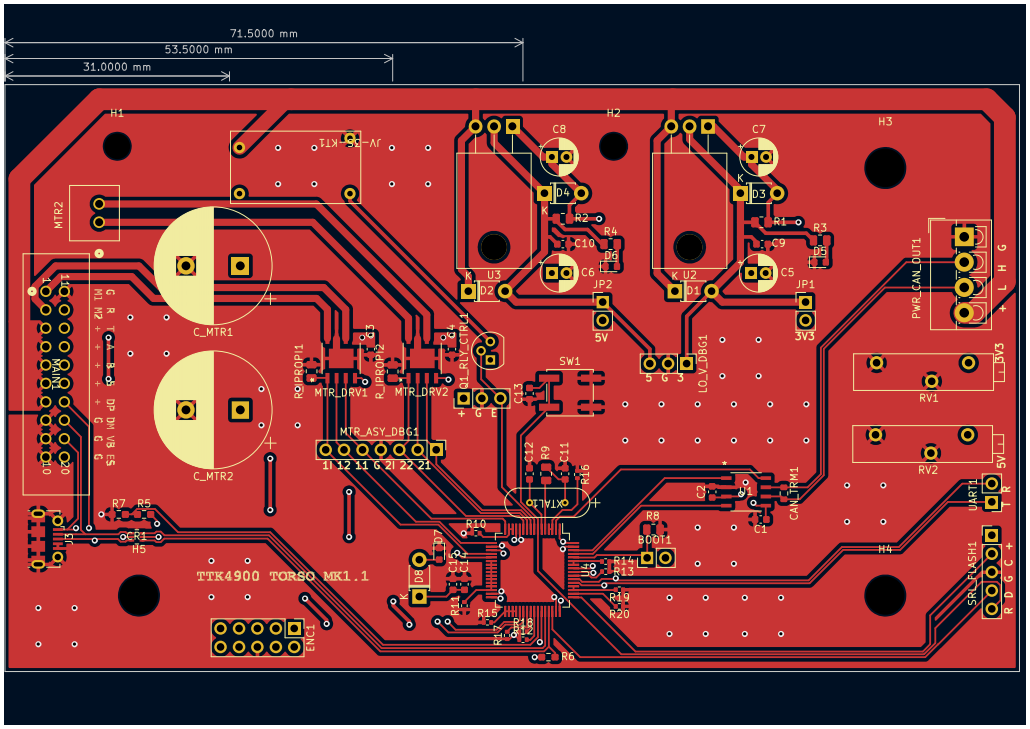

Figure 11: Front copper and silk layers of the improved torso board

[3]Investigation during the specialisation project suggested this was the system's original operating voltage.

MTR_ASY_DBG1	**Meaning**	**Q1_RLY_CTRL1**	**Meaning**
1I	DRV1 VIPROPI	+	3.3V
12	DRV1 PWM2	G	Ground
11	DRV1 PWM1	E	Relay enable
G	Ground	**LO_V_DBG1**	**Meaning**
2I	DRV2 VIPROPI	5	5V output
22	DRV2 PWM2	G	Ground
21	DRV2 PWM1	3	3.3V output
PWR_CAN_OUT1	**Meaning**	**SRL_FLASH1**[a]	**Meaning**
+	Sys voltage in	+	VDD Target
L	CANL line	C	Programmer clock
H	CANH line	G	Ground
G	Sys ground out	D	Programmer data
		R	Reset target

Table 8: Pin header legends for the torso control unit. [a]The flash header was designed for use with an ST-LINK programmer, and is described in chapter 6.2.4 of [16].

7.7 Shoulder

As shown in table 4, changes made in the torso control unit largely apply to the shoulder control unit as well. This section presents changes unique to the shoulder, illustrated in figure 12.

7.7.1 Mount points

Mount point H1 was moved 1mm to the right, and the diameter of all mount points were increased by 0.5mm compared to Mk1.

7.7.2 IMU

The Mk1 design contains an IMU board mounted on a hardpoint in the upper arm connected to the shoulder control unit via a set of wires similar to the hand control unit and lower arm IMU. The IMU was moved to the shoulder control unit itself in order to reduce overall system complexity by removing one PCB from the design. The IMU can be seen in the lower right of figure 12, between the MCU and encoder 2 connector pin header.

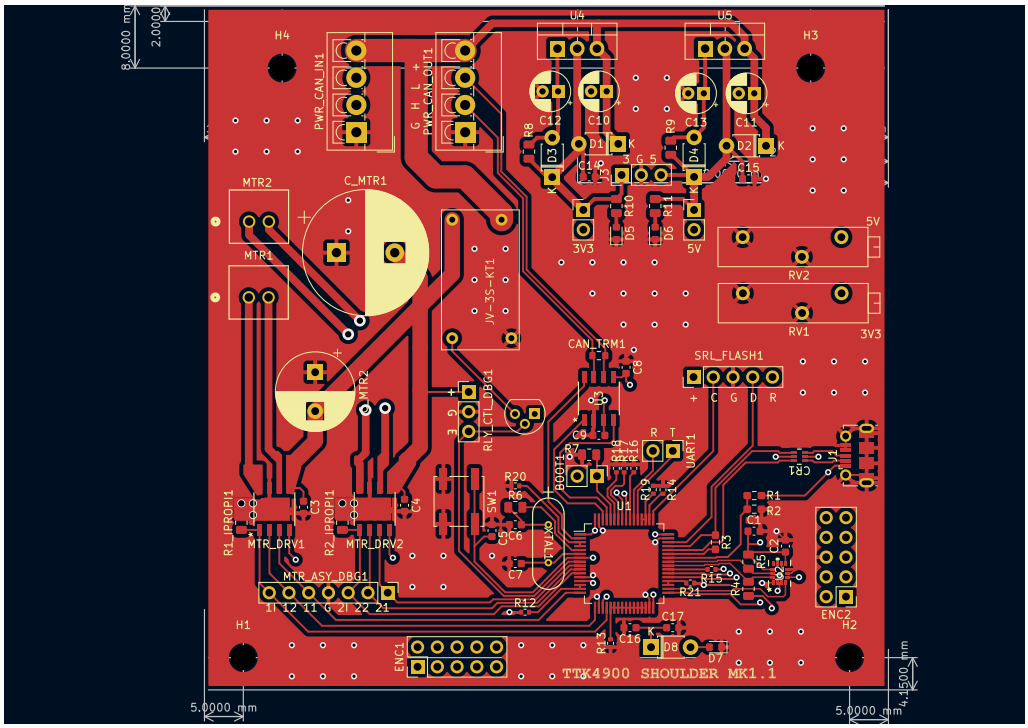

Figure 12: Front copper and silk layers of the improved shoulder board

7.8 Hand

The hand control unit could not be verified during the specialisation project due to a short circuit between the power input line and ground layer. The cause was found to be a misplaced stitching via, and care was taken to avoid this error in this and every other board produced afterwards. As the various subassemblies had largely been verified in the other control units, it was assumed that this was the only error preventing the hand unit from functioning correctly. Pin header legend for the hand control unit is presented in table 9, and boards are presented in figures 14 and 14.

7.8.1 Connector placement

Connector pin headers for the motors and CAN bus/power input were changed from the left to right hand side of the board in order to accommodate installation after the discovery was made that wires would not fit inside the hand chassis with the Mk1 design. Footprints were changed from horisontal to vertical for the same reason.

7.8.2 Board outline

Board outline was changed to accommodate vertical headers, expanding the board width by 2mm in that region. Additionally, it was discovered that wires for the the Hand B (optical sensor) would not fit. A 2mm tab was added in the top right corner to solve this issue.

7.8.3 Wire traces

The Mk1 version largely utilised the front copper layer for signal traces, causing most traces to run directly underneath the voltage regulators in the middle of the board. It was feared that noise from the regulators might disturb these signals. While no tests could be performed to verify this

concern due to the short circuit mentioned in section 7.8, most signals running the length of the board were moved to the back copper layer from an abundance of caution.

7.8.4 Encoder connector sockets

The hand encoders utilise a separate interface with the hand control units compared to the other encoders/control units in that their pins are inserted directly into the board rather than being routed through a 2x5 pin connector. The Mk1 connector sockets were found to be too tight for proper installation, and their diameter was increased from 1mm to 1.5mm.

7.8.5 Hand B: Optocoupler

The OPB971 optical sensor activates when its aperture is obstructed, such that a short circuit occurs between the output and ground pins. A voltage sensor placed between the output and voltage input pins will then sense the differential. A breadboard test was conducted around this concept with an LED placed between the input and output pins: when the aperture was obstructed, the LED lit. The optical sensor output pin was routed to a GPIO pin on the hand MCU on the assumption that it would act as a substitute for the LED, sensing the input/output differential upon activation of the optical sensor.

SRL_FLS_URT1	**Meaning**	**PWR_CAN_IMU1**	**Meaning**
+	VDD Target	+	5V output
C	Programmer clock	C	I2C clock
G	Ground	D	I2C data
D	Programmer data	G	Ground
R	Reset target	+	Input voltage
T	UART Tx	L	CANL
R	UART Rx	H	CANH
CON_A1	**Meaning**	G	Ground
+	5V output	**IMU_OPT1**	**Meaning**
O	Twist optical sensor	O	Wrist optical sensor
G	Ground	I	IMU interrupt

Table 9: Pin header legends for the hand control unit. **CAUTION:** The 5V output on the I2C header, adjacent to power input on the CAN/power header, MUST NOT have a voltage applied to it. As before, the symbols are to be interpreted as overlays of the pins.

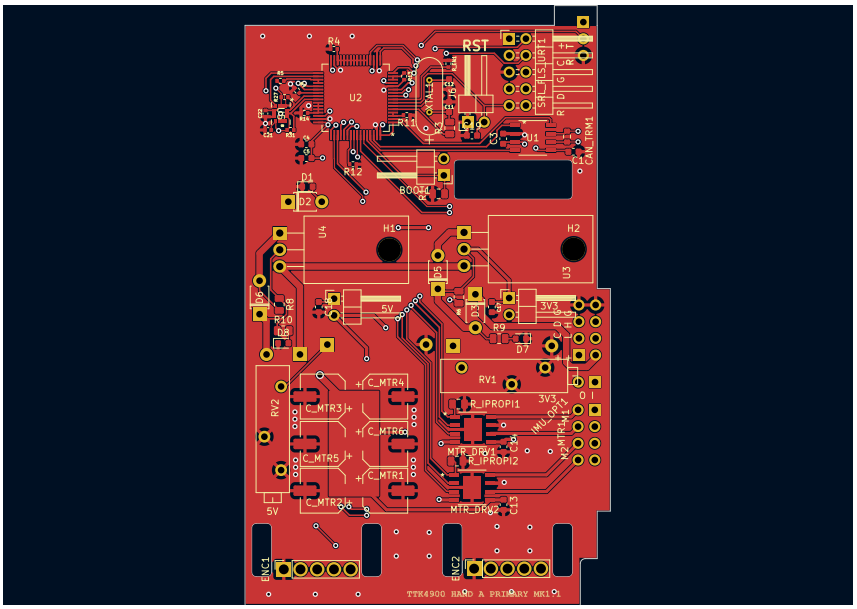

Front copper of the improved hand control unit

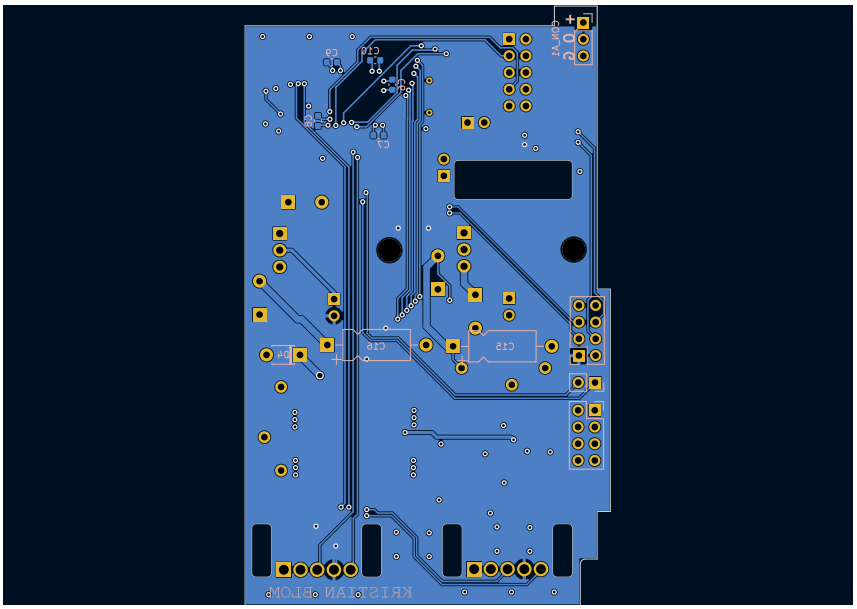

Back copper of the improved hand control unit

Figure 13: Front and back copper layers of the improved hand unit

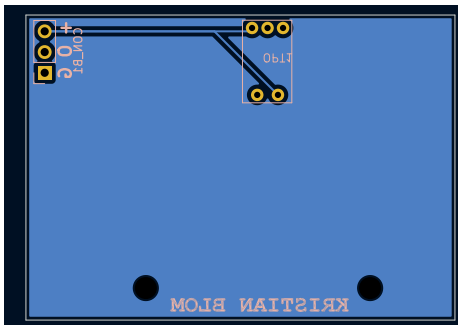

Figure 14: Back copper and silk layers of the hand B board

7.9 Verification

All PCBs were tested before installation into the arm before installation, similar to the specialisation project. They are presented in order of dependency on previously tested systems, sorted by assembly.

7.9.1 Voltage regulators

For each of the control units, voltage adjustment potentiometers RV1 and RV2 were turned until 3.3V and 5V were measured between ground and the relevant pin of LO_VLT_DBG1, see fig 24. Jumpers JP1 and JP2 were then connected with jumpers, and voltages were measured again to ensure no voltage drops, which would be indicative of a short circuit, were present. No voltage drops were measured, and the voltage regulators were judged to be operational.

7.9.2 MCU programming

The previously generated MCU pinout was compiled using VSCode and the ST extension (see section 6.1), and attempts were made to flash each of the control units also using the ST extension with the resultant binary file. This yielded no errors, effectively verifying the MCU voltage supply, serial/flash header designs, and the connection between the external computer and ST-LINK programming unit embedded in the Nucleo development kit. The MCUs were deemed operational.

7.9.3 Motor control relay, GPIO

The motor control relay makes an audible click when activated. The program mentioned in the previous test was expanded to include a simple loop activating and deactivating the relay every second by writing to the "RELAY_EN_PIN" on PC0. This tests the aliasing of GPIO pins to human readable names (see section 8.4), the transistor circuit, and the relay. Audible clicks were heard, and relay control was deemed operational. This test applies to the torso and shoulder control units, as the hand does not use a relay.

7.9.4 Motor drivers, PWM generation

PWM was tested using a test program from the specialisation project, updated to the Mk1.1 MCU pinout. The program generates a triangle wave at approximately 0.5Hz, which is used to scale the PWM duty cycle output from pins PA[2,3] and PC[1,2] (see section 8.8) for motor driver 1 and 2, respectively. The duty cycles must be inverse in order for the motor drivers to activate correctly, i.e. if PA2 has 40%DT, PA3 must have 60%DT, see datasheet[18] chapter 8.4.1. This test applies to all control units.

PWM output was verified by probing the MTR_ASY_DBG1 header, see fig 23, with an oscilloscope. PWM signals with waxing/waning duty cycles according to the generated triangle wave were observed for both motor drivers on all control units. The test was repeated for the motor driver output pins, and the PWM signals were observed here, too, at a voltage identical to the system input voltage of 20V[4].

Addressing the key improvement point from the specialisation project, no voltage was measured on the DRVn_IPROPI lines during this test. This implies that the discussed interference mode is not present in the current peripheral configuration, and the motor driver assemblies were deemed operational.

[4]The highest setting of the avaiable power supply

7.9.5 UART data transmission

UART transmission was tested by sending the character string "HELLO, WORLD!" using configuration parameters discussed in section 8.9 to the external computer via the Nucleo development kit's UART-to-USB adapter (see chapter 6.8 of UM1724[16]). The signal was listened for using PuTTy with configuration settings mirroring those of the MCU, and was received successfully from all control units.

UART reception was tested by activating the motor control relay upon reception of the character "R", detected via the UART reception interrupt handler. This was successful for the torso and shoulder control units. The hand control unit had no simple way to test reception, and this was assumed to be functional based on the results from the torso and shoulder units. UART data transmission was deemed operational.

7.9.6 Twist optical sensor

The twist optical sensor was tested by enabling an interrupt on PC11 upon a rising edge, and using sending a message over UART in the interrupt handler. The sensor was obstructed using a paper sheet, but no interrupt was triggered.

The error was found to be in the design of the sensor circuit. As mentioned in section 7.8, the optical sensor shorts its output pin to ground. Thus, the MCU will always measure 0V between output and ground. To amend this, two resistors of $10k\Omega$ were added between V_{cc} and OUT, OUT and Ground, respectively, of the Hand B connector pin header[5]. Before obstruction, the MCU will measure 2.5V, or half of the optical sensor V_{cc}, which is above the five volt tolerant pin activation threshold of 1.85V for a MCU supply voltage of 3.3V (MCU datasheet, table 66[15]). On obstruction of the sensor, the measured voltage will be 0V.

The interrupt was reconfigured to activate on a falling edge, and the test was repeated. The interrupt was triggered, and the optical sensor was deemed operational. This test applies to the hand control unit.

7.9.7 End switch and wrist optical sensors

The end switch and wrist sensors were tested by applying a 5V input voltage, and measuring the voltage between the OUT and ground pins when the switch was pressed/wrist joint manipulated to obstruct the sensor. Output voltage was found to be 2.7V. As discussed in section 7.9.6, this is above the five volt pin activation threshold, and the sensors were deemed to be operational.

7.9.8 I2C data transfer

I2C was tested by attempting to read the "WHO_AM_I" register of the three LSM6DSM IMU units[13] using a program developed for the specialisation project, and displaying the value via UART. The program utilises the STM32 HAL library discussed in section 8.1, which returns a status message of "HAL_ERROR" if a function fails in hardware. If the test is succesful, IMU assemblies, IMU boards and I2C peripheral configuration have been designed/assembled correctly.

The tests were generally not successful, and further testing was necessary to isolate the error(s). Several units were used in the process:

- Hand control unit: has one onboard IMU (IMU2) on I2C port 3, and one external IMU (IMU1) on I2C port 1.
- Shoulder control unit: has one onboard IMU (IMU0) on I2C port 3.

[5]Changing the PCB design itself was not deemed worth the time and money

- Breadboard IMU: an IMU on a breakout board, previously used for circuit design.
- IMU PCB 1: One copy of the IMU board design seen in figure 7, intended to function as IMU1.
- IMU PCB 2: Similar to IMU PCB 1, made for these tests.
- Adafruit unit: Adafruit MMA8451 accelerometer breakout[1], a COTS IMU bought for these tests, and to act as IMU board replacements should a solution not be found.
- Arduino UNO: Hobby/development kit for embedded programming, explicitly compatible with the Adafruit unit.

Attempts were made at reading the "WHO_AM_I" registers of all availabe IMUs, results presented in table 10.

IMU\MCU	**Hand I2C1**	**Hand I2C3**	**Shoulder I2C3**	**Arduino UNO**
Hand onboard	-	HAL_ERROR	-	-
Breadboard	WHO_AM_I	-	-	-
IMU PCB 1	HAL_ERROR	-	-	-
IMU PCB 2	HAL_ERROR	-	-	-
Shoulder onboard	-	-	WHO_AM_I	-
Adafruit	HAL_ERROR	-	-	WHO_AM_I

Table 10: Summary of attempts to read IMU registers

No debug headers were included in the I2C/IMU assemblies. Oscilloscope readings were therefore limited to Hand I2C1, where a breadboard was used to insert probes along the data and clock lines. Common for negative ("HAL_ERROR") results was that the waveform looked correct up until the point where a slave ACK (see 5.1) should have appeared. This indicates that the circuit is correctly designed, and that I2C1 is correctly configured (see 8.5).

Furthermore, the breadboard IMU worked with hand I2C1, and the shoulder onboard IMU worked with I2C3. This proves definitively that I2C peripherals are viably configured, and it strengthens the indication that circuit design is viable: Shoulder and hand onboard IMUs both use the IMU assembly schematic (fig 20), so any difference between the two would be limited to circuit layout. No noteworthy differences were found in the layout of the hand and shoulder onboard IMU circuits. The IMU assembly itself is based on the breadboarded design, which did also work.

One difference between the IMU PCB design (fig 19) and the IMU assembly is that both interrupt pins are never grounded at the same time, see equation 1. No indication was found that this would lead to undefined behaviour beyond a note that the output is "forced to ground" by default. See table 19 of the datasheet[13]. However, when the breadboard IMU circuit was modified to let one or both interrupt(s) float, communication with this unit failed, too. This indicates that the IMU board circuit design may need to be revisited.

All circuits except the Adafruit unit were hand soldered, and some difference in quality may be expected. Soldering was done by reflow oven and solder paste, and had generally been successful thus far in the project. However, due to its 14 pads at a pitch of 0.5mm in an LGA package, the LSM6DSM was significantly more difficult to solder than other ICs. Relevant solder points of MCUs and IMUs were inspected using a stereoscope, but no difference between functional and non-functional units could be established[6]. As a test for visual inspection, IMU board was resoldered with a deliberately uneven amounts of solder paste on the IMU pads. The IMU was clearly tilted after soldering, but there was no indication of short circuiting between pads with too much paste. However, pins with very little paste appeared to have been disconnected as the IMU tilted. None of these clues to improper connections could be seen in the other units[7]. The MCUs were also inspected, and I2C pins appeared to be in order. At this point, six IMUs had been soldered with

[6]No figures could be acquired from the stereoscope

[7]Getting a clear view of the connection was difficult in all cases, which in itself may be a source of error

only two positive results. Considering that all were soldered with little variation in process, it seems improbable that the soldering process should be the only cause of the negative results.

An attempt was made at establishing whether the IMUs themselves may be defunct. This was initially assigned a very low probability considering the effect it would have on ST's business model should it routinely ship defunct batches of ICs, but one result lends the hypothesis credibility: An attempt at reading the shoulder onboard IMU's Z axis acceleration, it failed. Reading other axes, both acceleration and rotation rate, was successful. No further tests could be made to establish whether the remainder of the batch was defunct.

The Adafruit units which were supposed to act as a replacement for the IMU boards also failed when paired with hand I2C1. It is assumed to be because the MMA8451 requires a repeated start condition when initialising communication with the master (Overview chapter[1]). While the STM32F303 is configurable for repeated start condition (chapter 25.2.1 of UM1786[14], this was not implemented due to time constraints.

Summarised:

- The I2C peripheral configuration is viable.
- The IMU assembly circuit is not incorrect.
- The IMU board design may need revisiting – grounding both interrupt pins.
- The soldering process may need to be revisited.
- Two axes are available on the shoulder joint: X and Y.

I2C data transfer was deemed minimally operational.

7.9.9 USB data transfer

Didn't work, lost motivation due to time and UART working.

7.9.10 CAN bus data transfer

In order to verify CAN bus, the hand control unit was programmed to send a CAN message to the torso control unit upon activation of the twist optical sensor via the interrupt handler. The torso control unit was programmed to send a message over UART upon reception of a CAN message from the hand unit. The twist joint was then moved to the position where the sensor should activate. A message was read in PuTTy, and CAN bus was deemed operational.

7.9.11 verification summary

- Voltage regulators correctly output 3.3V and 5V.
- MCUs may be programmed via the Nucleo devkit ST-LINK programmer.
- Motor control relays correctly function as a dead man's switch.
- Motor drivers are controllable via PWM.
- Information may be exchanged with the arm via UART.
- Twist and end stop sensors are operational and in use.
- Wrist sensor is operational, but not in use.
- One of three IMUs are partially operational.

- USB was dropped due to complexity and time, lack of need.
- Information may be exchanged between control units via CAN bus.

7.10 Installation

7.11 Circuit diagrams

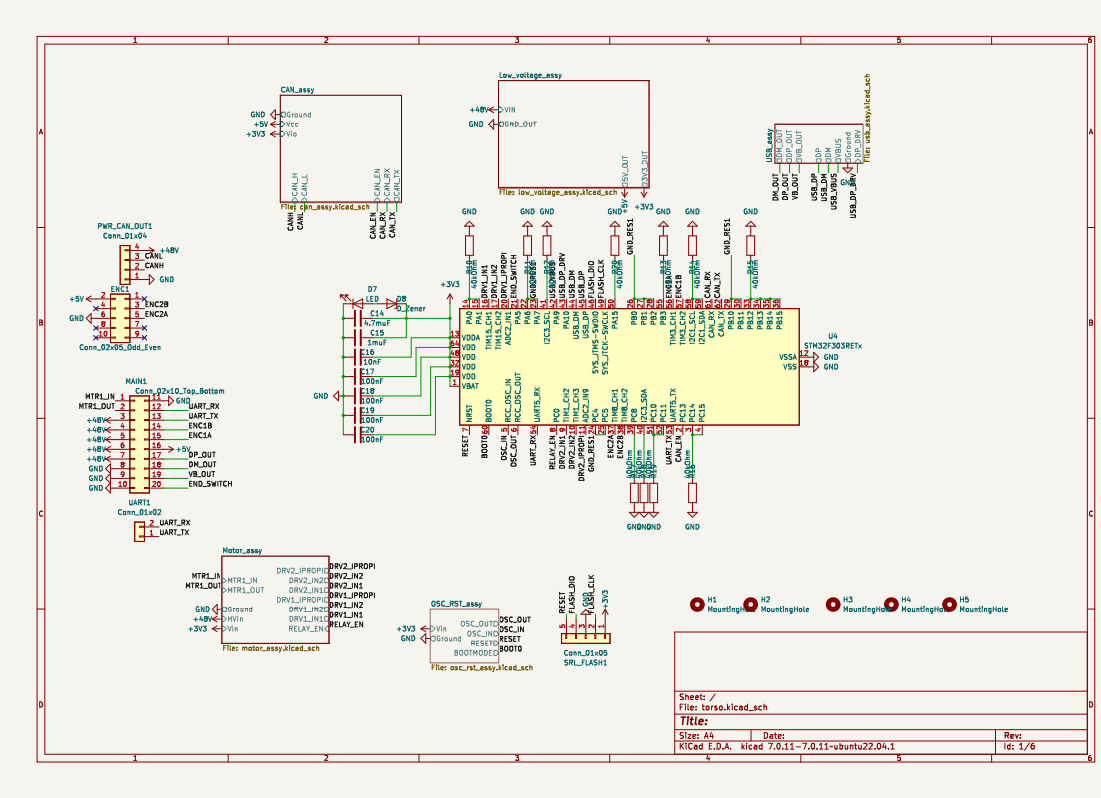

Figure 15: Circuit diagram of the Mk1.1 torso control unit

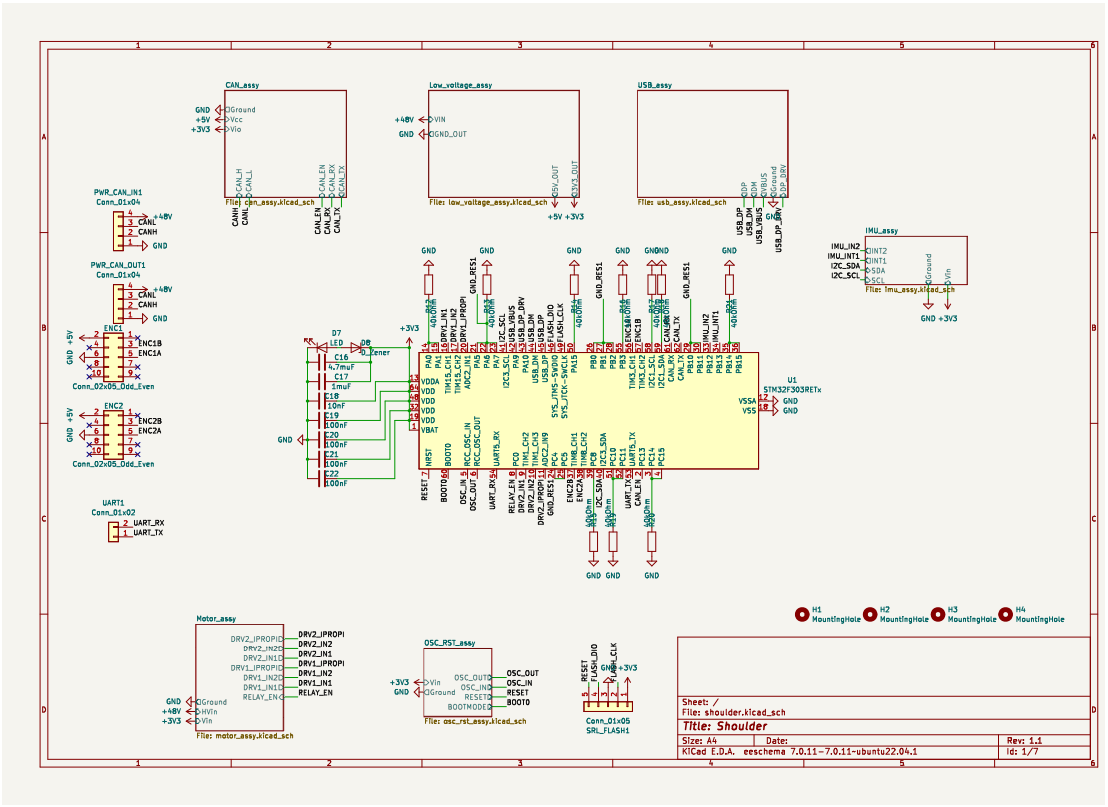

Figure 16: Circuit diagram of the Mk1.1 shoulder control unit

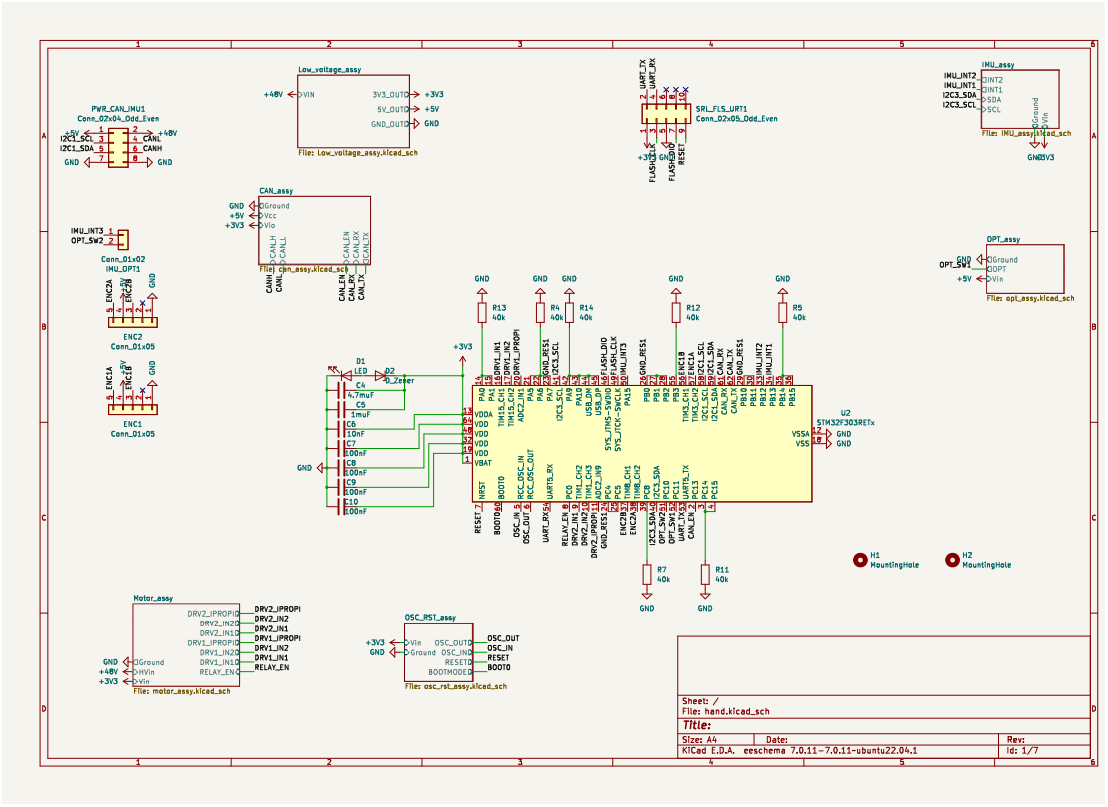

Figure 17: Circuit diagram of the Mk1.1 hand control unit

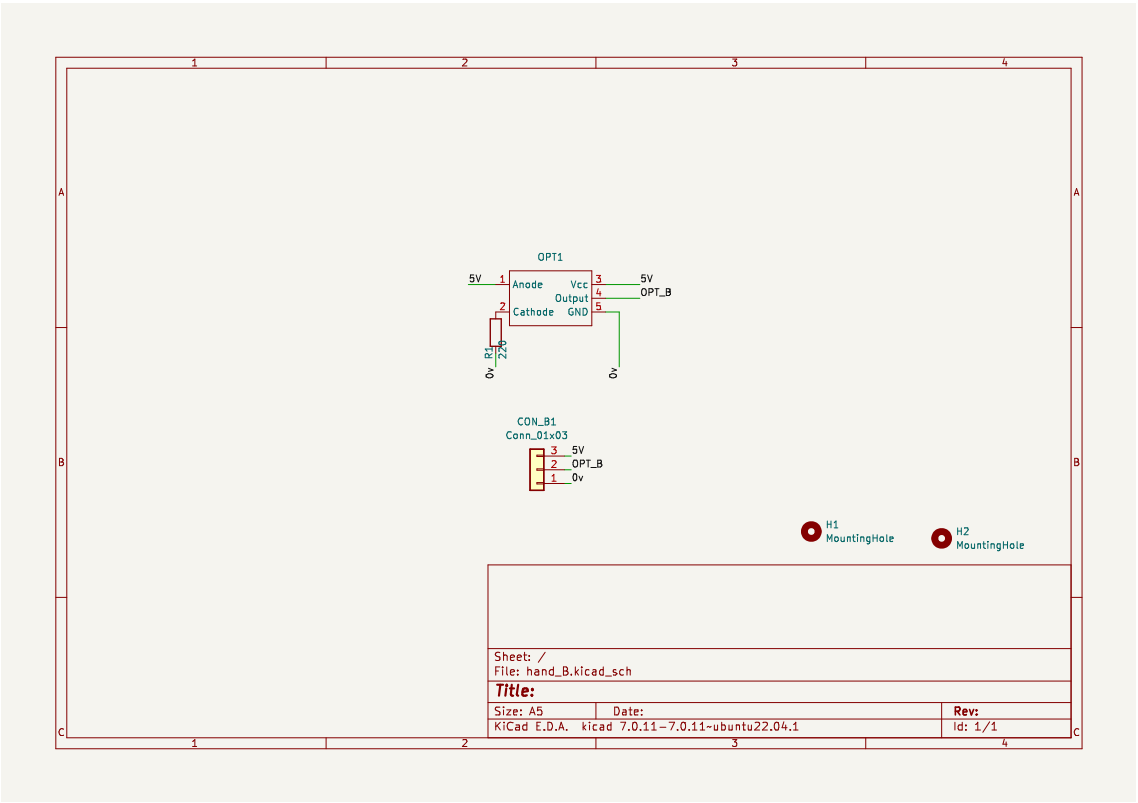

Figure 18: Circuit diagram of the twist optical sensor

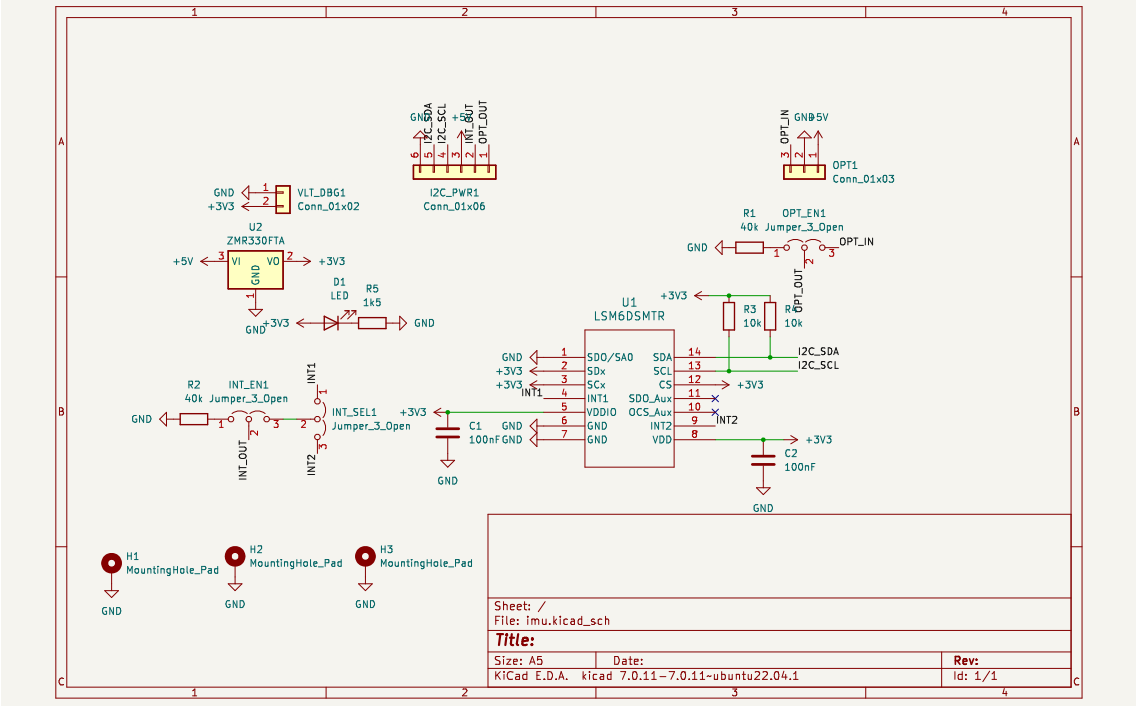

Figure 19: Circuit diagram of the Mk1.1 IMU board

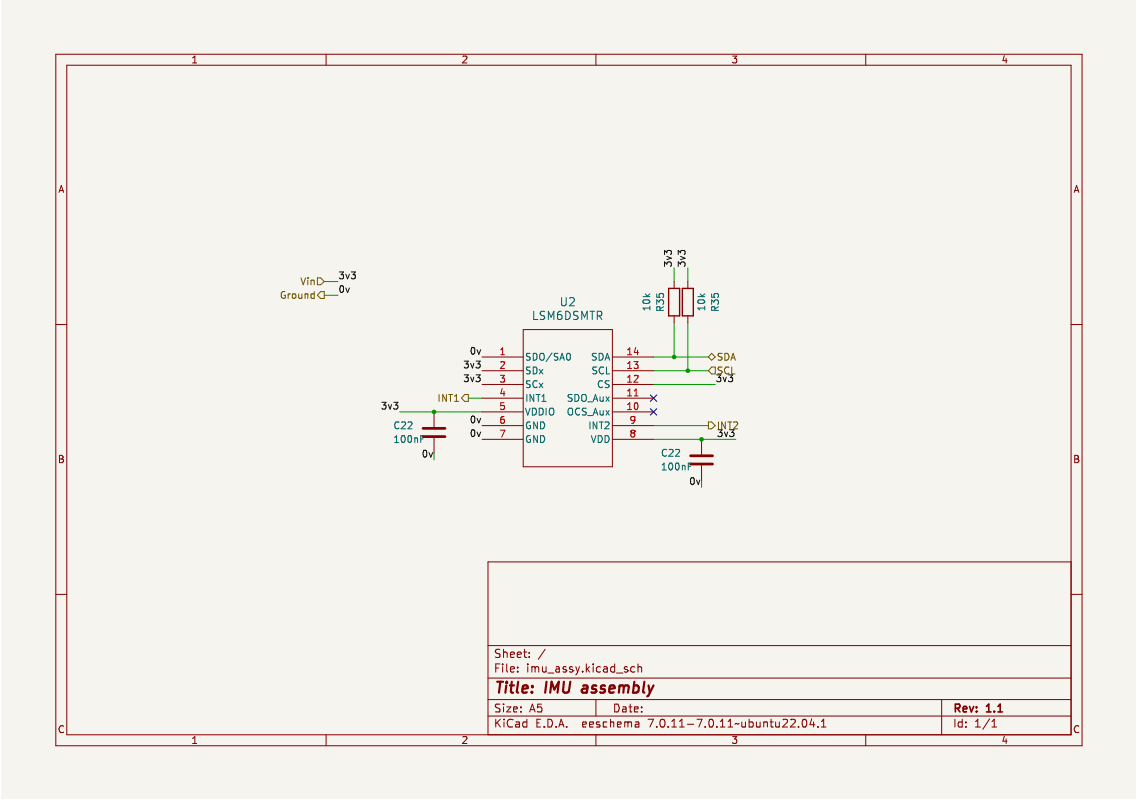

Figure 20: Circuit diagram of the Mk1.1 IMU assembly, present in the IMU board, shoulder and hand control units

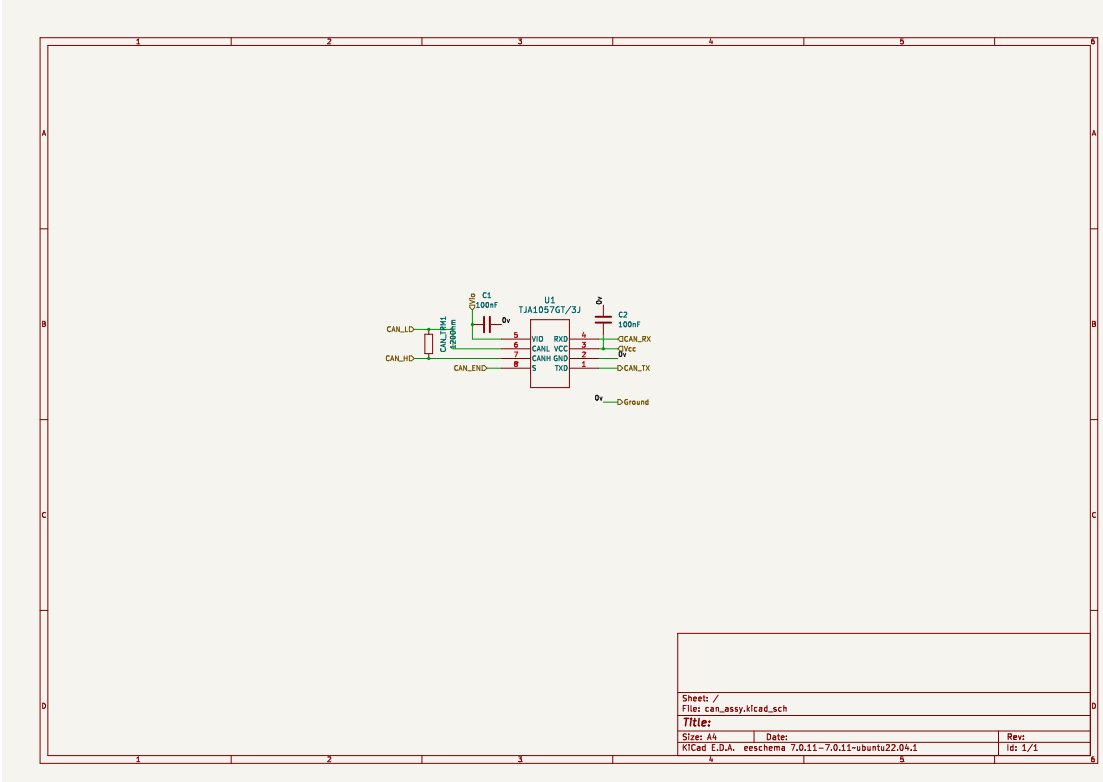

Figure 21: Circuit diagram of the Mk1.1 CAN assembly, present in the hand control unit

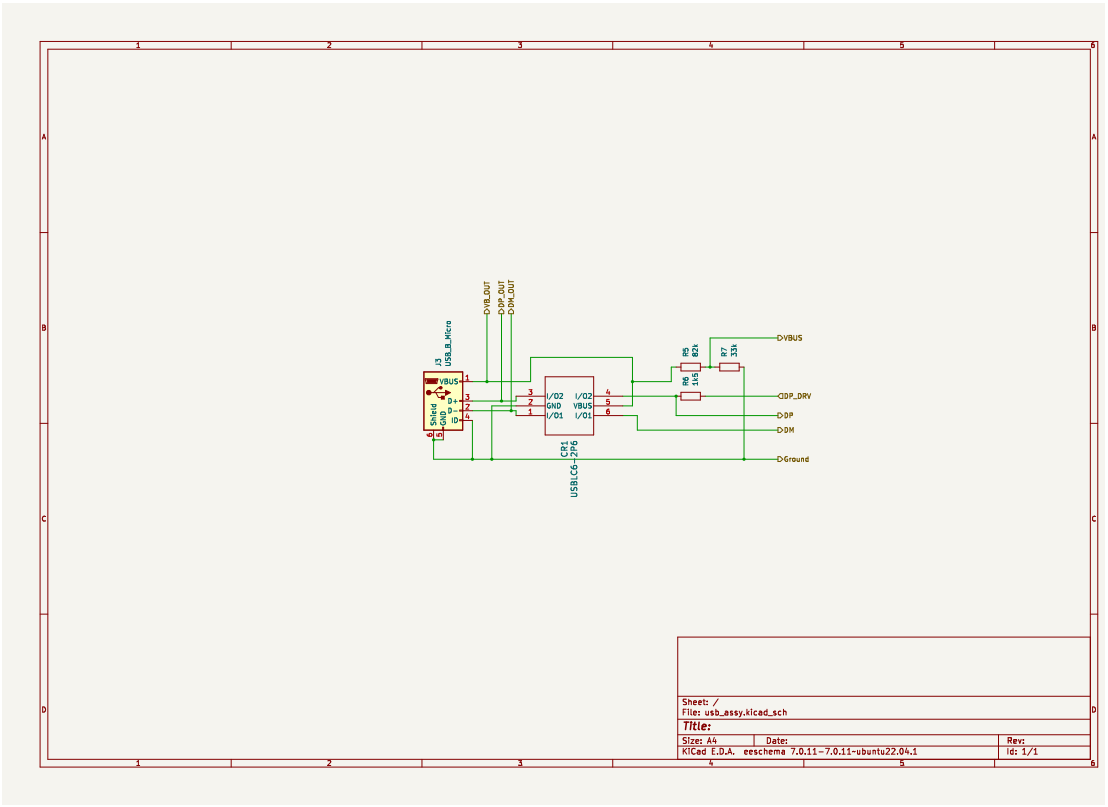

Figure 22: Circuit diagram of the Mk1.1 USB assembly, present in the torso and shoulder control units

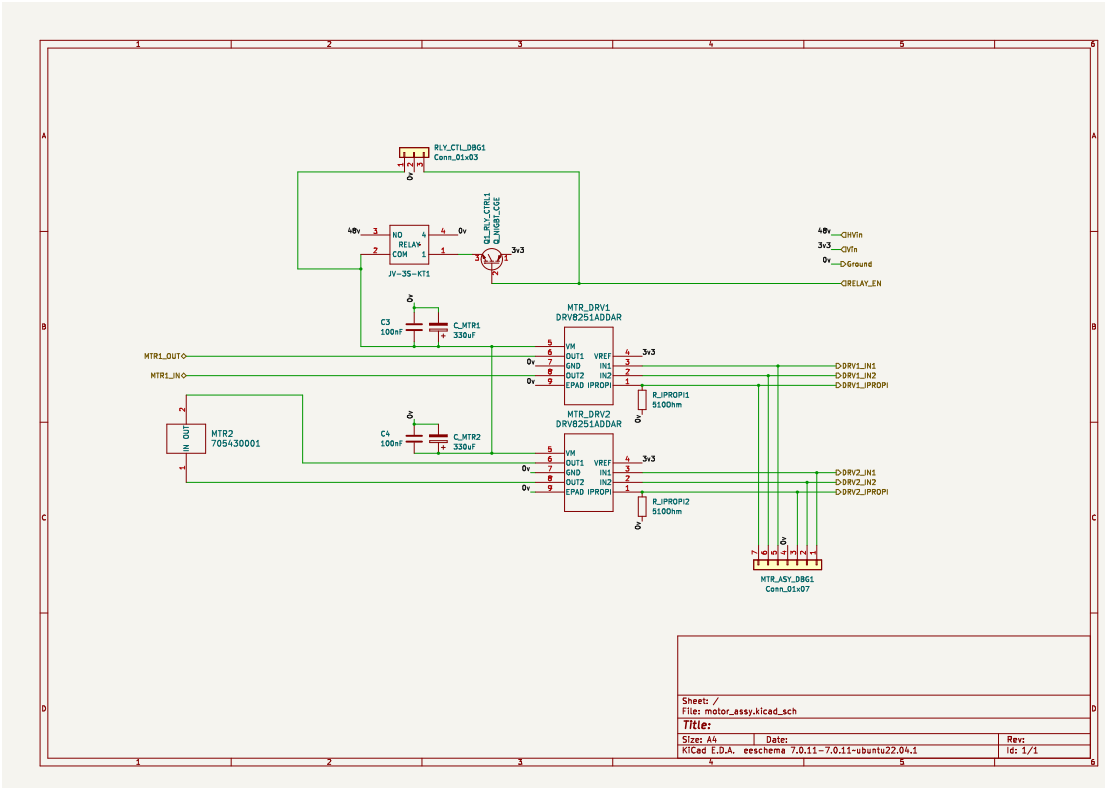

Figure 23: Circuit diagram of the Mk1.1 motor driver assembly, present in the control units

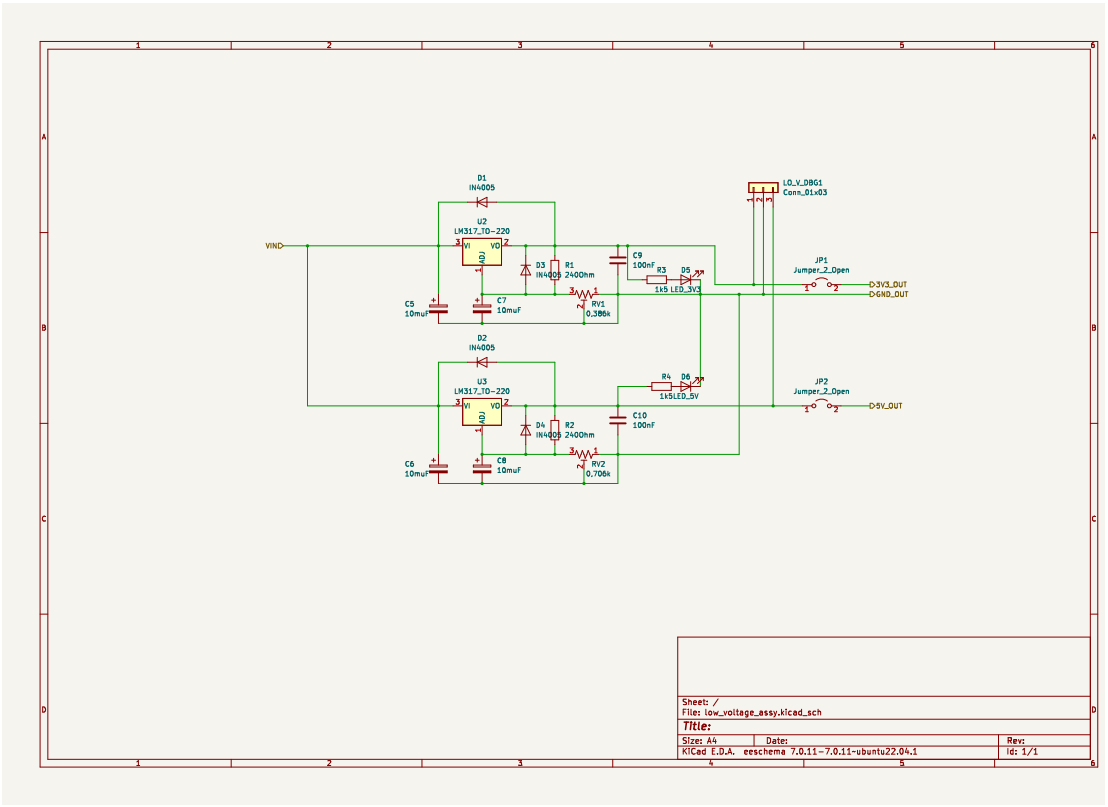

Figure 24: Circuit diagram of the Mk1.1 voltage regulator assembly, present in the control units

8 Peripheral configuration

Done in CubeMX, which generates a set of files in a generated folder structure. Peripheral usage dictate higher level architecture.

8.1 STM32F303 overview

General overview, HAL explanation

8.2 ADC

8.3 CAN

8.4 GPIO

8.5 I2C

8.6 Interrupts

Probably a lot of references to architecture here

8.7 SYS

Arguably not a peripheral, includes clocks etc

8.8 Timers

8.8.1 Encoder timers: TIM3, TIM8

8.8.2 PWM generators: TIM1, TIM15

Duty cycle frequency, noise

8.8.3 Interrupt timers: TIM2, TIM4, TIM7

8.9 USART

8.10 USB

9 Software architecture

9.1 General considerations

Low coupling between modules to simplify maintainability. Developing software around hardware; embedded programming. Naming conventions

9.2 Arm onboard

Input: UART/USB Structure: Peer-to-peer vs master/slave? MCUs are equal, but torso deals with external comms. Backbone: CAN bus Module inclusion: Preprocessor statements Folder structure: CubeMX vs TTK4900 ROS vs Terminal USB vs UART Timer based interrupts

9.3 ROS nodes

10 Hardware drivers

Point out that these are the TTK4900 drivers, not CubeMX generated files. Not including joint controllers, can executives; these are control system domain. Defining positive and negative direction for the joints, make figures

11 Control system

Main loop, joint controllers, can executives, state machine

12 Calibration

Method of calibration, usage in the state machine.

13 ROS nodes

14 Tests

Message round trip times: CAN, I2C, accelerometers=(CAN+I2C)

15 Results

Regret not putting indicator LEDs on GPIO, would have made basic testing easier. The optical sensor shenanigans could have been avoided if the original sensors had been studied more carefully. State machine is whack, inconsistent calibration for twist for whatever reason Accelerometers are whack, should have had proper debug headers System works well overall when accelerometers are disabled ROS is really powerful, and can probably be expanded readily CAN bus craps out for voltages above 25V

The decision to place the upper arm IMU on the shoulder control unit PCB made it impossible to debug, and may be considered a violation of the project's second goal (or requirement number NUMBER) as the whole board will need to be replaced in order to repair/replace the IMU.

USB non-functional. Could it be due to the clamping voltage in the rail TVS? Or not implementing VBUS ESD protection properly, see an4879 2.3.

Input voltage no more than 25V, far less than the suggested 48V. Heat, motor control, CAN bus.

Low coupling between modules? Not really, look at the include graph

Were the ARs adhered to? More or less

16 Discussion

Pros and cons of using youtube as a source: bootstrap large project, making other people's mistakes. Not having access to a debugger was frustrating

17 Conclusion

18 Operations

Bibliography

[1] Adafruit. *Adafruit MMA8451 Accelerometer Breakout*. 2023.

[2] Kristian Blom. *From hardware to control algorithms: Retrofitting a legacy robot using open source solutions*. 2023.

[3] Bourns. *CDSC706-0504C - Surface Mount TVS Diode Array*. 2015.

[4] TT Electronics. *Photologic® Slotted Optical Switch OPB960, OPB970, OPB980, OPB990 Series*. 2019.

[5] Escap. *escap 23LT12 graphite/copper commutation systems*. 2024.

[6] U. Ghia, K. N. Ghia and C. T. Shin. 'High-Re Solutions for Incompressible Flow Using the Navier-Stokes Equations and a Multigrid Method'. In: *Journal of Computational Physics* 48 (1982), pp. 387–411.

[7] DIODES incorporated. *ZMR series: fixed 2.5, 3.3 and 5 volt miniature voltage regulators*. 2013.

[8] Pittman Metek. *Brush commutated DC motors DC030B Series*. 2024.

[9] Pittman Metek. *Brush commutated DC motors DC040B Series*. 2024.

[10] Pittman Metek. *Brush commutated DC motors DC054B Series*. 2024.

[11] NXP. *TJA1057 High-speed CAN transceiver*. 2023.

[12] ST. *AN4879: Introduction to USB hardware and PCB guidelines using STM32 MCUs*. 2023.

[13] ST. *LSM6DSM iNEMO inertial module: always-on 3D accelerometer and 3D gyroscope*. 2017.

[14] ST. *ST UM1786: Description of STM32F3 HAL and low-layer drivers*. 2020.

[15] ST. *STM32F303xD STM32F303xE*. 2016.

[16] ST. *UM1724: User manual STM32 Nucleo-64 boards (MB1136)*. 2020.

[17] Avago Technologies. *HEDS-9000/9100 Two Channel Optical Incremental Encoder Modules*. 2016.

[18] TexasInstruments. *DRV8251A 4.1-A Brushed DC Motor Driver with Integrated Current Sense and Regulation*. 2022.

[19] TexasInstruments. *LMx17HV High Voltage Three-Terminal Adjustable Regulator With Overload Protection*. 2015.

Appendix

A Hello World Example

```cpp
int main {
    // This is a comment
    std::cout << "Hello World from C++!" << std::endl;
    std::cout << "I am using the default style to print this code in beautiful
    ↪  colors. Since the text is so long I have to include the 'breaklines'
    ↪  option as well" << std::endl;
    return 0;
}
```

⋮

```python
# This is a comment
print('Hello world from Python!')
print('I am using the "rrt" style to print this code in beautiful colors')
```

⋮

```matlab
% This is a comment
disp("Hello World from MATLAB!");
disp("I am using the "tango" style to print this code in beautiful colors");
```

B Flow Chart Example

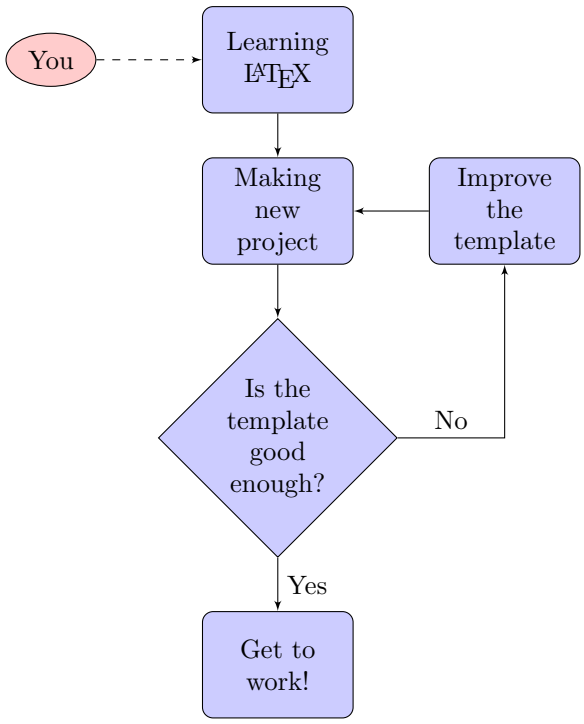

C Sub-figures Example

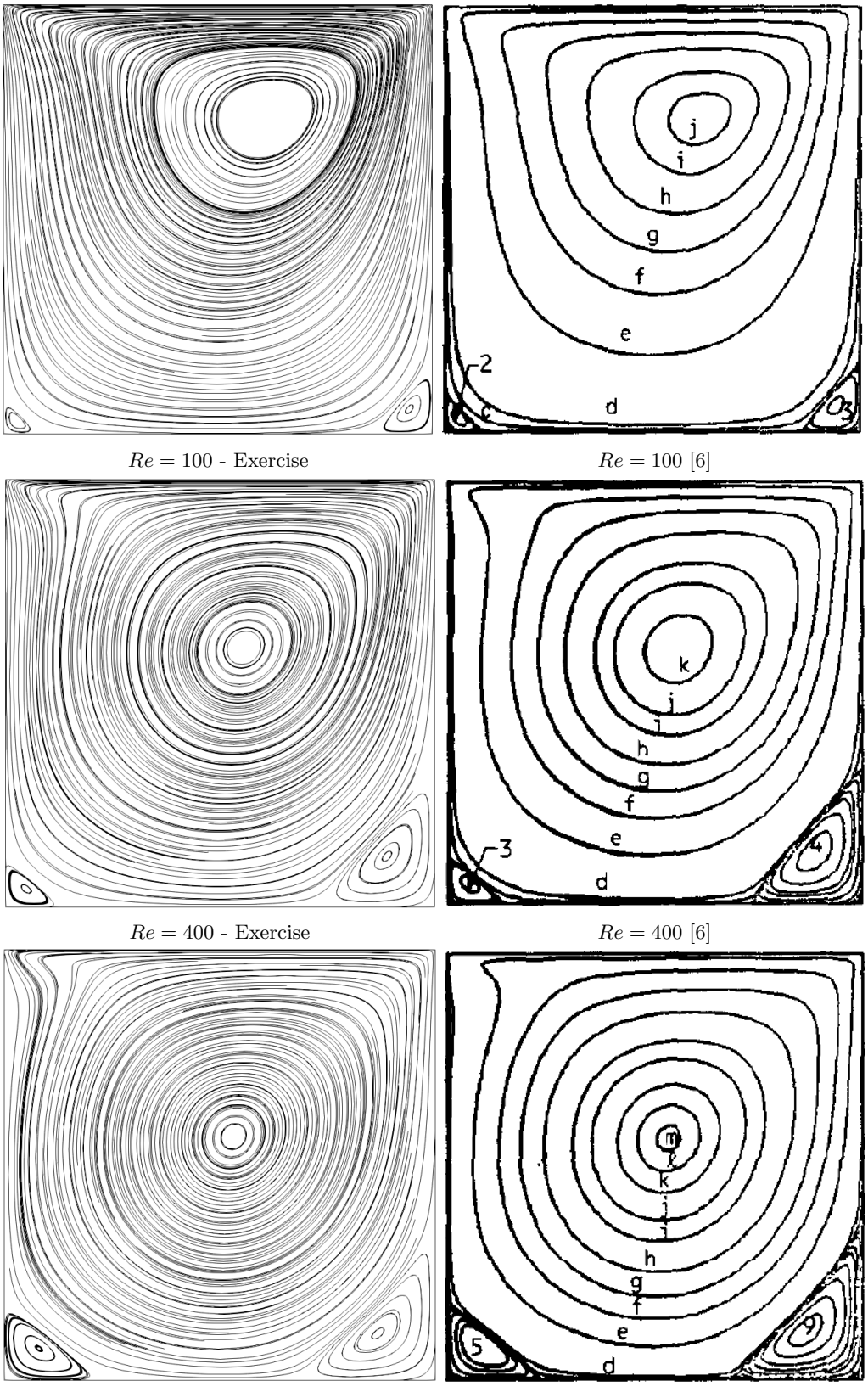

$Re = 100$ - Exercise $Re = 100$ [6]

$Re = 400$ - Exercise $Re = 400$ [6]

$Re = 1000$ - Exercise $Re = 1000$ [6]

Figure 25: Streamlines for the problem of a lid-driven cavity.